Review

Modified Half-Titanocenes as Polymerization Catalysts: Basic Concept, Displayed Promising Characteristics and Some Mechanistic Insights

Kotohiro Nomura * and Ketsanee Jantawan

Posted Date: 28 January 2026

doi: 10.20944/preprints202601.2232.v1

Keywords: titanium catalysts; polymerization; polyolefin; copolymerization; half-titanocene; homogeneous catalysts; XANES; EXAFS; ethylene

 doi:10.20944/preprints202601.2232.v1

Review

Modified Half-Titanocenes as Polymerization Catalysts: Basic Concept, Displayed Promising Characteristics and Some Mechanistic Insights

Kotohiro Nomura * and Ketsanee Jantawan

Department of Chemistry, Tokyo Metropolitan University, Hachioji, Tokyo, 1920397, Japan

* Correspondence: ktnomura@tmu.ac.jp

Abstract

Development of new polymers, that cannot be achieved by using conventional catalysts has been the central research objective, and copolymerization is an effective strategy to modify the materials' (thermal, physical, mechanical and electronic) properties. Modified half-titanocenes, Cp'TiX_2(Y) (Cp' = cyclopentadienyl; X = Cl, Me etc.; Y = anionic donor such as phenoxide, ketimide, amidinate etc.), are known to be the effective catalysts. This review introduces several selected efforts for efficient synthesis of ethylene copolymers containing cyclic olefins, biobased conjugated dienes, disubstituted α-olefins including effect of cocatalysts. Moreover, here introduces analysis using XAS (X-ray absorption spectroscopy), which has been recognized as powerful method providing direct information of the catalytically active species, such as coordination numbers and the distances of the coordinated atoms as well as oxidation state and the geometry of the metal centre in catalyst solution.

Keywords: titanium catalysts; polymerization; polyolefin; copolymerization; half-titanocene; homogeneous catalysts; XANES; EXAFS; ethylene

1. Introduction

Polyolefins [linear high density polyethylene (HDPE), linear low density polyethylene (LLDPE), low density polyethylene (LDPE), and isotactic polypropylene (PP)] are the dominant commodity thermoplastics, accounting for over 50% of global plastic production in the world; the growth of the world production still has been observed especially in Asia [1]. Transition metal catalyzed olefin coordination insertion polymerization is the key technology for the industrial production [2–8]. The development of new polymers, that cannot be achieved by using conventional catalysts (such as Ziegler-Natta, metallocene catalysts), has been considered as the central research objective [2–6,9–23]. Copolymerization has been taken into consideration as an effective strategy, because their thermal, physical, mechanical and electronic properties of the resulting copolymers can be modified by the individual components, incorporation of two (or three) monomer units [4,6,14–17]. Design, development of the molecular catalysts, that display highly active with better comonomer incorporations, has thus been the pivotal challenge [2–23].

Discovery of metallocene catalysts (called single-site catalysts), bearing two cyclopentadienyl (Cp') ligands of type Cp'$_2$MX_2 (M = Ti, Zr, Hf; X = halogen etc.), marked an importance of the catalyst design, since the resultant copolymer possesses uniform composition with controlled molecular weight due to the formation of single active species in the catalytic polymerization [5,9–12]. The fact displayed a different feature in the copolymerization using the Ziegler-Natta catalysts (called multi-site catalysts), which generate several catalytically active species *in situ*; as a results, Ziegler-Natta catalysts afford the copolymer with multiple compositions [5,9–12]. The high oxidation state cationic alkyl species, Cp'$_2$M$^+$R (R = alkyl), formed by treating with borate or methylaluminoxane (MAO) through alkyl abstraction, have been proposed as the active species in this catalysis (Scheme

 doi:10.20944/preprints202601.2232.v1

1) [5,9–17,24–27]. In this catalysis, nature of the active species, such as basic geometry, electronic and steric bulk of the ligand sets, directly affects the catalytic activity, stereo specificity, and the comonomer incorporation in the copolymerization.

It is widely recognized in ethylene copolymerization with α-olefin that bridged (*ansa*, linked) metallocene catalysts generally showed better α-olefin incorporation than the unbridged analogues; the fact was explained as due to different coordination environment imposed by the bridging framework (Scheme 1) [5,9–17,28,29]. Accordingly, linked (*ansa*, bridged) half-titanocenes exemplified as constrained geometry catalyst (**CGC**), [$Me_2Si(C_5Me_4)(N^tBu)$]$TiCl_2$ [12,13,28–33], exhibit enhanced ability in α-olefin incorporation in the copolymerization. Interestingly, **CGC** exhibited styrene incorporation in the ethylene copolymerization, although the incorporation level typically remains below 50 mol% [33–35]. This limitation was later overcome by the bimetallic system (**bimetallic CGC**, Scheme 1), which enabled synthesis of the copolymer with high styrene content (76 mol%) [21,22,36,37].

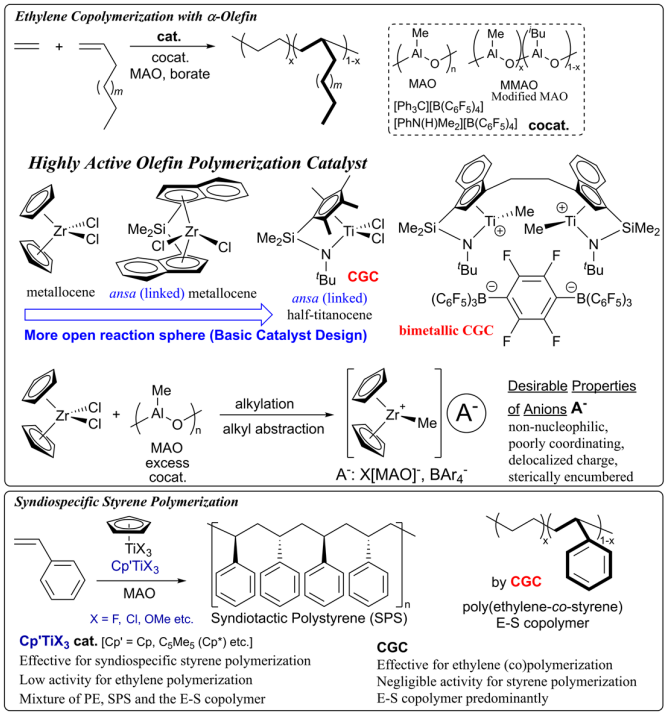

Scheme 1. Group 4 transition metal complex catalysts for olefin polymerization and syndiospecific styrene polymerization (SSP).

In contrast, it has been widely known that ordinary half-titanocenes containing one Cp' of type, $Cp'TiX_3$, are effective catalysts for synthesis of syndiotactic polystyrene (SPS, Scheme 1), that is inaccessible by conventional radical, ionic (anionic, cationic) polymerization [38–40]. However, these $Cp'TiX_3$ catalysts generally display low catalytic activity for olefin polymerization, and the (attempted) ethylene/styrene copolymerization yielded a mixture of polyethylene, SPS, and the copolymer in small amount [34,41]. The behaviour displays the sharp contrast from the facts that **CGC** and ordinary metallocene catalysts showed the negligible catalytic activities [34,36,37]. Moreover, as described above, **CGC** predominantly produce the ethylene/styrene copolymers [33–37]; these facts led to an assumption that the active species in olefin polymerization differ from those in the syndiospecific styrene polymerization, as described in detail below.

It is well known that modified half-titanocenes featuring anionic donor ligands, $Cp'TiX_2(Y)$ (Scheme 2, Y = phenoxide, ketimide, amidinate, phosphinimide, iminoimidazolide, iminoimidazolidide etc.) [6,14–17], first introduced by our team [42,43], display remarkably

 doi:10.20944/preprints202601.2232.v1

distinctive catalytic properties, particularly in the copolymerization of ethylene (or propylene, α-olefin) with sterically encumbered olefins, cyclic olefins, and with aromatic vinyl monomers (Scheme 2) [14–17]. The phenoxide (**1**) [42–45] and the ketimide (**2**) [46–52] catalysts have proven distinctively effective for synthesis of new (co)polymers [6,14–17]; it has become clear that effective catalyst for the targeted (co)polymerization can be finely tuned through modification of cyclopentadienyl (Cp') and the anionic donor (Y) ligands. Later, the η^1-amidinate analogue (**3**) [4,53–55] enabled industrial-scale production of ethylene propylene diene terpolymer (EPDM) [4], as chlorine-free synthetic rubber without deep cooling, characteristic of conventional (Ziegler type) vanadium-based catalyst systems, therefore highlighting the practical significance of this catalyst platform [37]. Moreover, interestingly, the phenoxide catalysts exhibit remarkable activities for SSP [56,57], and exclusively afforded ethylene/styrene copolymers in the copolymerization [56,58]. Moreover, these catalysts enabled synthesis of a series of ethylene copolymers with the other aromatic vinyl monomers (Scheme 2) [59]. The observed characteristics represent quite different from those observed by metallocene and linked half-titanocene catalysts.

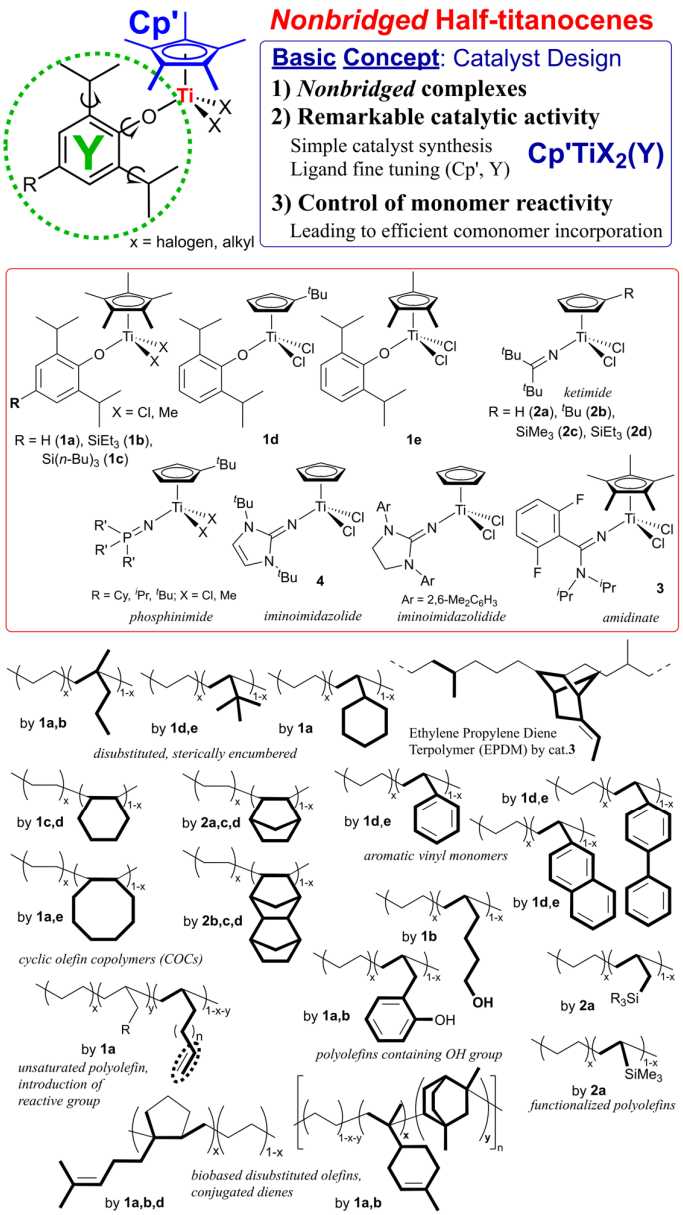

Scheme 2. *Nonbridged* half-titanocenes: Basic catalyst design and selected examples of catalysts, copolymers.

 doi:10.20944/preprints202601.2232.v1

This review thus introduces several selected recent efforts for synthesis of ethylene copolymers containing cyclic olefins [60–68], biobased conjugated dienes [69,70], disubstituted α-olefins [44,71–74] including effect of cocatalysts [75]. Moreover, here also introduces analysis results by synchrotron XAS (X-ray absorption spectroscopy) [27,76,77] which has been recognized as useful to obtain information not only of valence (oxidation state) and the basic structure (geometry) through XANES (X-ray Absorption Near Edge Structure), but also number of coordination atoms and the distance to the cantered metal through EXAFS (Extended X-ray Absorption Fine Structure) analysis.

2. Efficient Synthesis of Cyclic Olefin Copolymers (COCs)

Certain amorphous cyclic olefin copolymers (COCs) are polymeric materials with high transparency in the UV-vis region, thermal resistance (possessing high glass transition temperature, T_g), humidity resistance (negligible water absorption), low dielectric constants, and then dimensional stability [78–86], as commercialized as TOPAS® [87] and APEL® [88], ethylene-based copolymers with norbornene (NBE) and tetracyclododecene (TCD), respectively, for optical lens and films for medical applications. There have been extensive number of reports for ethylene/NBE copolymerization using group 4 transition-metal complexes, including metallocenes [89–95], bridged half-metallocenes (so-called constrained geometry type) [96–99], modified non-bridged half-metallocenes [60–63], and the others called post metallocene catalysts [100–105]. However, reports for the efficient synthesis of high molar mass the ethylene/NBE copolymers possessing high T_g values (high NBE contents) with efficient and random NBE incorporation remain scarce [61,63], Moreover, vanadium-based catalyst systems, such as $VOCl_3$ or $VO(OEt)Cl_2$ together with $EtAlCl_2$·Et_2AlCl cocatalyst, which have been employed in the commercial production of ethylene/TCD copolymers, require deep-cooling conditions because of limited thermal stability of these catalyst systems [106]. The efficient synthesis of high molar mass ethylene/TCD copolymers still have been limited by the ketimide analogue [63,64], whereas copolymerization employing conventional metallocene catalysts [107–110] and the known linked half-titanocene catalyst (**CGC**) [64] generally suffers from low catalytic activity and/or inefficient TCD incorporation. The catalyst development for synthesis of high molecular weights COCs possessing high glass transition temperature maintaining promising optical property (birefringence, with low water absorption, dielectric constants, and dimensional stability) has been an attractive subject [78–86].

As described above, ethylene/NBE copolymers are known to be commercialized COC, as TOPAS® [87], using metallocene–MAO catalysts (Scheme 3). In general, the copolymerization by ordinary metallocenes (**SBI-Zr**) and linked half-titanocene catalysts (**CGC**) afforded amorphous poly(ethylene-*co*-NBE)s with uniform compositions possessing a sole glass transition temperature (T_g) by DSC thermograms [79–85]. However, both the activity and the M_n values in the resultant copolymers decreased upon increase in the NBE/ethylene feed molar ratios (increasing the NBE concentration charged and/or lowering ethylene pressure) [89–99], as exemplified in Table 1 [61,82]. The fluorenyl-substituted CGC (**Flu-CGC**) enables living NBE polymerization in the presence of dried MAO or MMAO (obtained as white solid by removal of $AlMe_3$ and Al^iBu_3 from the commercially available samples) with much improved NBE incorporation [99]; the resultant copolymers with α-olefins (1-octene, 1-decene, and 1-dodecene) possessed gradient NBE incorporation (monomer sequences in the copolymers) due to different reactivity between two monomers [6,84].

 doi:10.20944/preprints202601.2232.v1

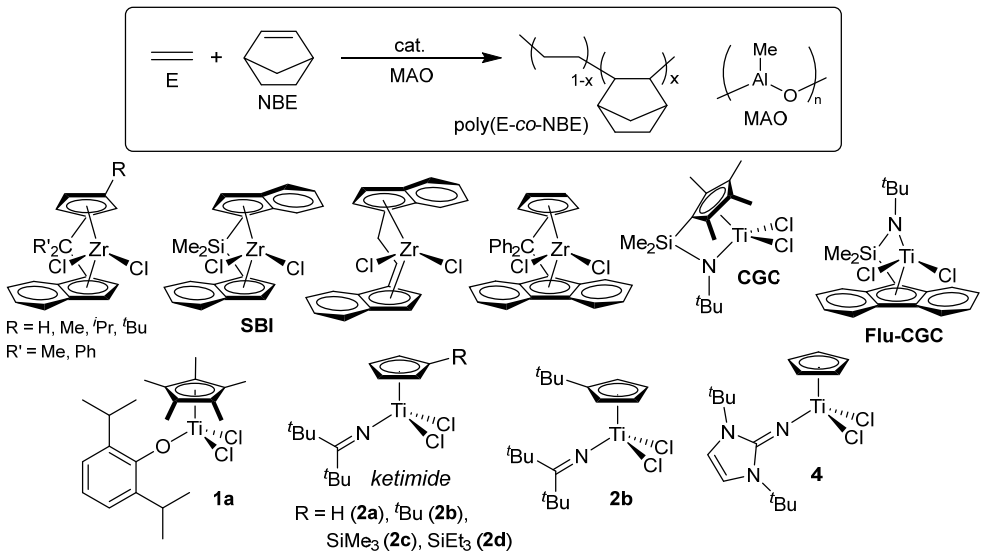

Scheme 3. Ethylene copolymerization with norbornene (NBE).

The ketimide-modified half-titanocene, $CpTiCl_2(N=C^tBu_2)$ (**2a**, Scheme 3) first demonstrated efficient synthesis of ethylene random copolymers with high NBE contents possessing high M_n values (Table 1) [61]. The activities (productivities) did not change significantly even over 30 min and increased at elevated temperature (60 ºC); the copolymerization conducted at 80 ºC did not show the significant decrease in the activity [61]. In contrast to the observation in the copolymerization using the metallocene, **CGC** catalysts, the activity by **2a**–MAO catalyst rather increased upon increase in the initial NBE feed concentration, the catalyst afforded the high molar mass copolymers [61]; Al cocatalyst (MAO, MMAOs) does not significantly affect the activity and the NBE incorporation. Therefore, this catalysis method using **2a** gave the high molar mass copolymers with high NBE contents (58.8-73.5 mol%, Table 1) with uniform compositions [61]. A linear correlation between the T_g values and the NBE content in the copolymers was demonstrated even at high NBE contents, strongly suggesting the NBE random incorporation. The random NBE incorporation was also demonstrated by their microstructural analyses of the copolymers, consisting of NBE isolated, alternating, repeat incorporation without stereoregularity [6,61,63,80,82].

Table 1. Ethylene (E) copolymerization with norbornene (NBE) by $[Me_2Si(indenyl)_2]ZrCl_2$ (**SBI**), $[Me_2Si(C_5Me_4)(N^tBu)]TiCl_2$ (**CGC**), $Cp'TiCl_2(N=C^tBu_2)$ [Cp′ = Cp (**2a**), $^t BuC_5H_4$ (**2b**), $Me_3SiC_5H_4$ (**2c**), $Et_3SiC_5H_4$ (**2d**)], and $CpTiCl_2[1,3\text{-}^tBu_2(CHN)_2C=N]$ (**4**)–MAO catalysts (in toluene, ethylene 2 or 4 atm, 10 min) [61–63].[a]

cat. (μmol)	temp. / ºC	E / atm	NBE[b] / M	activity[c]	M_n[d] ×10^{-4}	M_w/M_n[d]	T_g[e] / ºC	NBE[f] / mol%
SBI (0.10)	25	4	0.2	28900	23.1	2.02		10.8
SBI (0.10)	25	4	1.0	4860	22.9	2.37		29.5
CGC (0.50)	25	4	0.2	2460	21.1	1.88		9.6
CGC (0.50)	25	4	1.0	2000	12.8	2.15		26.5
2a (0.02)	80	4	1.0	133000	33.8	2.34		61.7
2a (0.02)	60	4	1.0	194000	47.5	2.20		51.2
2a (0.02)	40	4	1.0	48900	62.0	2.37		45.9
2a (0.02)	25	4	1.0	40200	71.9	2.92		40.7
2a (0.02)[g]	25	4	1.0	59700	61.3	2.18		41.0
2a (0.01)[h]	25	2	2.5	90000	32.3	2.09		58.8
2a (0.01)[h]	25	2	5.0	85800	34.0	2.00		65.8
2a (0.01)[h]	25	2	10.0	31500	44.4	2.01		73.5
2b (0.01)[i]	25	4	1.0	68400	62.4	2.78		38.2

 doi:10.20944/preprints202601.2232.v1

2b (0.10)[i]	25	4	5.0	15000	17.5	2.05		52.7
2c (0.02)[i]	25	4	1.0	28300	79.5	1.82	99.6	36.2
2c (0.05)[i]	50	2	6.0	32700	55.2	2.04	238	72.7[j]
2d (0.01)[i]	25	4	1.0	49800	82.9	2.06	94.1	37.5[j]
2d (0.01)[i]	50	4	1.0	91400	110	1.94	113	42.1[j]
4 (0.20)	25	4	1.0	6180	108	2.53		31.4
4 (0.20)	80	4	1.0	5780	80.0	2.35		36.9

[a]Conditions: Toluene+NBE total 50 mL, d-MAO 0.5-3.0 mmol. [b]Initial NBE feed conc. (mmol/mL). [c]Activity in kg-polymer/mol-M·h (M = Ti, Zr). [d]GPC data in *o*-dichlorobenzene *vs* PS stds. [e]By DSC thermograms. [f]NBE content (mol%) estimated by ^{13}C NMR spectra. [g]Time 30 min. [h]Toluene+NBE total 10 mL. [i]Toluene+NBE total 30 mL. [j]Estimated on the basis of the plots of T_g and NBE content.

The imidazolin-2-iminato modified half-titanocene, $CpTiCl_2$[1,3-^{t}Bu$_2$(CHN)$_2$C=N] (**4**), also exhibited promising capabilities in the copolymerization, probably due to the strong σ-donating nature. The catalyst (**4**) showed high catalytic activity affording high molar mass copolymers with rather efficient NBE incorporation as well as uniform composition [65]. The activities by **4** were rather low compared to the ketimide analogue (**2a**) and further ligand modification might be required, suggesting that the anionic donor ligand play an important role toward both the catalytic activity and the NBE incorporation.

More recently, as summarized in Table 1, improved both catalytic activities and NBE incorporation from the above ketimide catalyst (**2a**) could be achieved by introduction of trialkylsilyl group on the cyclopentadienyl fragment, (RC$_5$H$_4$)TiCl$_2$(N=C^{t}Bu$_2$) [R = SiMe$_3$ (**2c**) SiEt$_3$ (**2d**)]. These catalysts displayed remarkable activities (25700-91400 kg-polymer/mol-Ti·h) in the copolymerization at 50 ºC to afford high molar mass copolymers with high NBE contents (NBE 36.2-72.7 mol%) possessing high T_g value (238 ºC) [63]. The observed results seem interesting contrast to those in copolymerization using the *tert*-BuC$_5$H$_4$ analogue (**2b**, Table 1).

As described above, ethylene/TCD copolymers are known to be commercialized COC, as APEL® [88], which have been produced using vanadium-based catalyst systems ($VOCl_3$–$EtAlCl_2$·Et_2AlCl etc.) under deep-cooling conditions [106]. It seemed that the conventional (metallocene, linked-half-titanocene) catalysts face difficulty for synthesis of the high molar mass ethylene/TCD copolymers at moderate temperature (>50 ºC, Scheme 4) [107–110].

The ketimide-modified half-titanocene, (^{t}BuC$_5$H$_4$)TiCl$_2$(N=C^{t}Bu$_2$) (**2b**), demonstrated synthesis of the copolymers with remarkable activities (43700 kg-polymer/mol-Ti·h) to afford the copolymers possessing high T_g values (108-203 ºC) with uniform compositions (Scheme 4, Table 2) [64]. The Cp analogue (**2a**) showed lower catalytic activity than **2b**, and the M_n value in the resultant copolymer was low compared to that prepared by **2b** under the same conditions; modification of cyclopentadienyl fragment thus plays a key role [64]. The imidazolin-2-iminato analogue (**4**) also displayed rather low capability for the copolymerization [64]. The ketimide analogue seems to be thus promising for synthesis for COCs.

More recently, as seen in the ethylene/NBE copolymerization, the catalyst capability could be improved by introduction of trialkylsilyl group on the cyclopentadienyl fragment, (RC$_5$H$_4$)TiCl$_2$(N=C^{t}Bu$_2$) [R = SiMe$_3$ (**2c**) SiEt$_3$ (**2d**), Table 2] [63]. In particular, the SiEt$_3$ analogue (**2d**) showed higher catalytic activities at 50 °C, affording the high molecular weight copolymers with uniform composition possessing sole T_g values. The TCD contents in the copolymer increased with increase in the TCD concentration charged (as well as lowering the ethylene pressure), and these catalysts (**2c**,**d**) demonstrated synthesis of the copolymers with TCD content higher than 50 mol% (T_g = 255 °C, TCD 52.3 mol%) [63]. The results clearly indicate that further improvement in the catalyst capability can be achieved by the ligand modification.

 doi:10.20944/preprints202601.2232.v1

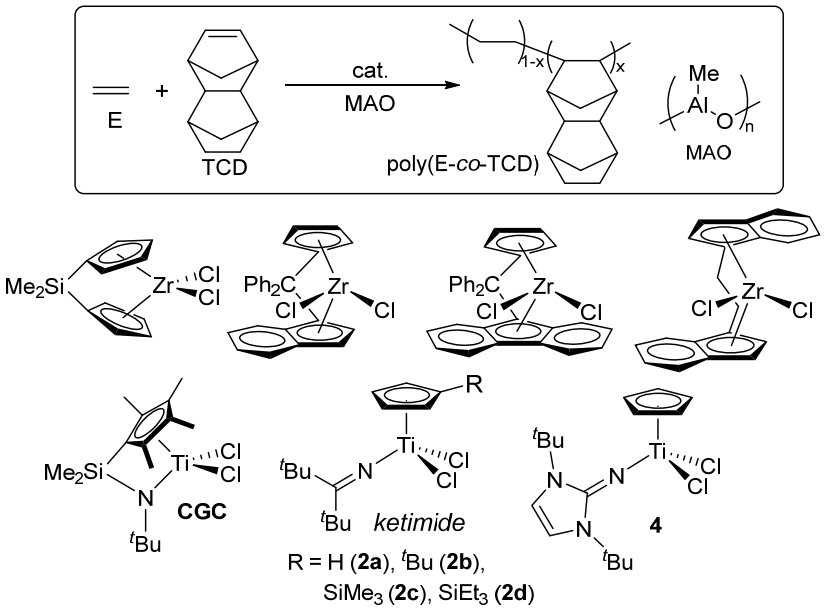

Scheme 4. Catalysts reported for ethylene copolymerization with tetracyclododecene (TCD).

Table 2. Ethylene copolymerization with tetracyclododecene (TCD) by $Me_2Si(C_5Me_4)(N^tBu)]TiCl_2$ (**CGC**), $Cp'TiCl_2(N{=}C^tBu_2)$ [Cp′ = Cp (**2a**), $^tBuC_5H_4$ (**2b**), $Me_3SiC_5H_4$ (**2c**), $Et_3SiC_5H_4$ (**2d**)]–MAO catalysts (in toluene, ethylene 4 or 6 atm, 10 min) [63,64].[a]

cat. (μmol)	E / atm	TCD[b] / M	temp. / ºC	activity[c]	M_n[d] ×10^{-5}	M_w/M_n[d]	T_g[e] / ºC	TCD[f] / mol%
CGC (0.05)	6	1.0	25	13900	14.3	1.58	56	
2a (0.80)	6	2.0	25	1650	1.92	1.41	150	
2b (0.02)	6	1.0	25	43700	5.88	1.60	108	25.6
2b (0.02)	6	2.0	25	23900	6.38	1.50	153	32.8
2b (0.02)	6	2.0	40	27800	6.43	1.67	170	33.5[g]
2b (0.02)	6	2.0	60	33300	6.53	1.72	177	35.3
2b (0.02)	6	3.0	25	16800	6.43	1.61	171	33.6[g]
2b (0.02)	6	4.0	60	22400	6.08	1.61	203	36.7
2c (0.02)	6	1.0	25	33400	17.3	2.03	102	23.7[g]
2c (0.05)	6	4.0	25	7710	6.41	2.03	202	42.5[g]
2c (0.10)	4	4.0	50	2560	3.90	1.95	255	52.3[g]
2d (0.02)	6	1.0	25	55900	7.29	1.88	119	26.9[g]
2d (0.04)	6	4.0	25	15700	5.40	2.41	203	41.9
2d (0.10)	4	2.0	50	9550	5.76	1.53	186	38.3
2d (0.20)	4	3.0	50	7790	3.98	1.72	234	48.3[g]
2d (0.10)	4	4.0	50	3790	2.79	1.79	244	50.3[g]

[a]Polymerization conditions: Toluene and TCD total 30 mL, d-MAO 3.0 mmol. [b]Initial TCD concentration in mmol/mL. [c]Activity = kg-polymer/mol-Ti·h. [d]GPC data in *o*-dichlorobenzene *vs* PS standards. [e]By DSC thermograms. [f]TCD content (mol%) estimated by ^{13}C NMR spectra. [g]Estimated based on the plots of T_g and TCD content.

Basic structure (size, strain etc.) in cyclic olefin directly affects not only the efficiency of cyclic olefin incorporation in the (ethylene) copolymerization, but also the properties in the resultant COCs (thermal and tensile properties, dielectric constant etc.) [6,84]. As described in the introduction, limited number of reports were known for successful synthesis of (rather high molar mass) amorphous ethylene copolymers with so called low strained cyclic olefins such as cyclohexene (CHE) [66,68], cycloheptene (CHP) [66,67], and *cis*-cyclooctene (COE) [66,67]. Recently, as shown in

 doi:10.20944/preprints202601.2232.v1

Scheme 5, synthesis of a series of amorphous ethylene and propylene copolymers with CPE, CHE, CHP, COE, tricyclo[6.2.1.0(2,7)]undeca-4-ene (TCUE), and with TCD were demonstrated [66,67]. Linear relationships between the T_g values and the cyclic olefin contents were demonstrated in all cases. These results thus strongly suggest that T_g values were affected by the cyclic structure in COCs (except the copolymers with CPE, COE). The T_g values in the propylene copolymers in the region of low cyclic olefin content (up to 25 mol%) seemed rather high compared to those in the ethylene copolymers [66]. This is due to rather high T_g value in the atactic polypropylene.

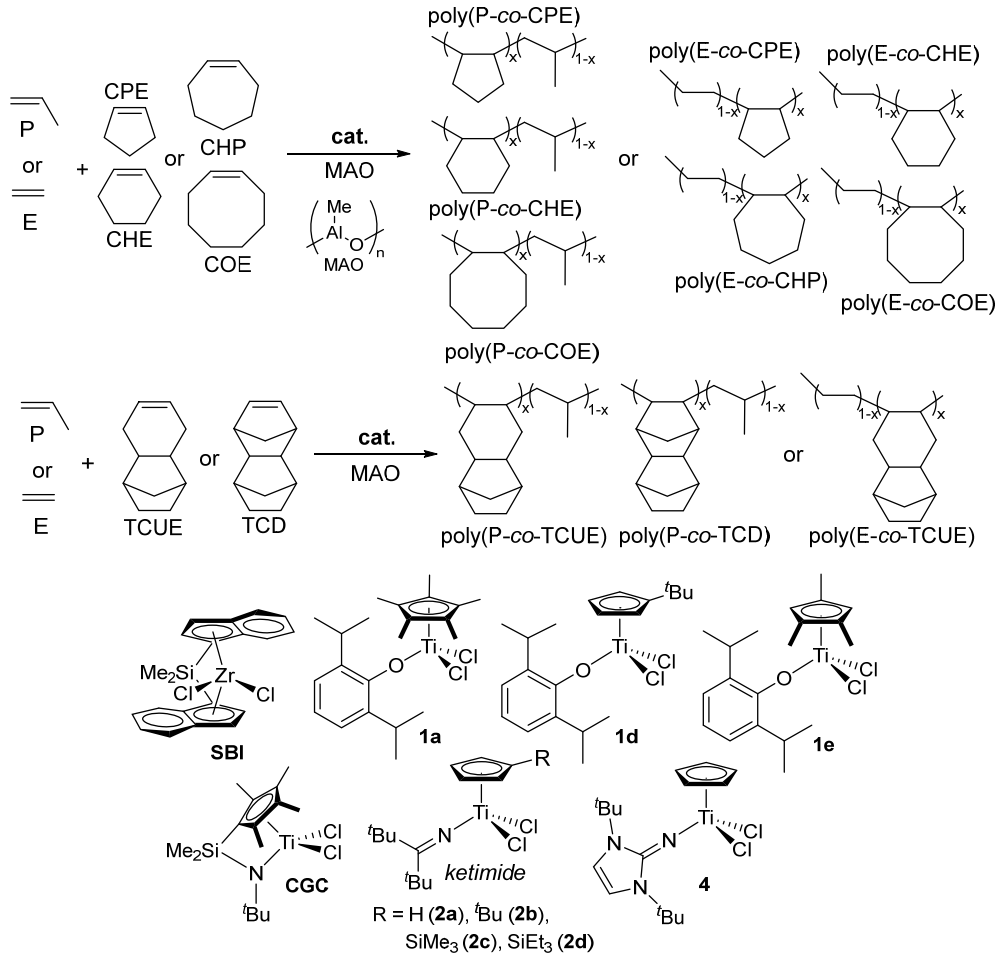

Scheme 5. Propylene or ethylene copolymerization with (low strained) cyclic olefins [66–68].

The cyclic olefin copolymers by copolymerizing norbornene (NBE) and tetracyclododecene (TCD) with various linear α-olefins, such as 1-hexane (HX), 1-octane (OC), and 1-dodecene (DD), using ketimide half-titanocene catalysts Cp'TiCl$_2$(N=C^{t}Bu$_2$) [Cp' = or Cp (**2a**), ^{t}BuC$_5$H$_4$ (**2b**)] (Scheme 6) [65]. The Cp analogue (**2a**) exhibited superior to the ^{t}BuC$_5$H$_4$ derivative (**2b**), exhibited over 10 times higher activity and more efficient comonomer incorporation under same condition. While these half-titanocene catalysts successfully produced high molecular weight TCD/α-olefins copolymers [65]. The conventional metallocene and **Flu-CGC** failed to synthesize the high molecular weight copolymers, yielding only low molecular weight oligomers [111–114].

A critical finding in this copolymer system is the linear relationship observed between the cyclic olefin content and glass transition temperature across all synthesized polymers. In copolymers with TCD exhibited higher T_g values than their NBE counterparts at equivalent cyclic olefin concentrations (exceeding 200 °C). The T_g values are further influenced by the α-olefins chain length, decreasing in the order of 1-hexene > 1-octene > 1-dodecene. Additionally, the reactive functionality was

 doi:10.20944/preprints202601.2232.v1

demonstrated by introducing via the incorporation of 1,7-octadiene (OD), which adds terminal olefinic double bonds to the side chains. In this term, the ^{t}BuC$_5$H$_4$ analogue (**2b**) proved more suitable than Cp analogue (**2a**) because the latter caused unwanted isomerization of the terminal double bonds into internal olefins [65].

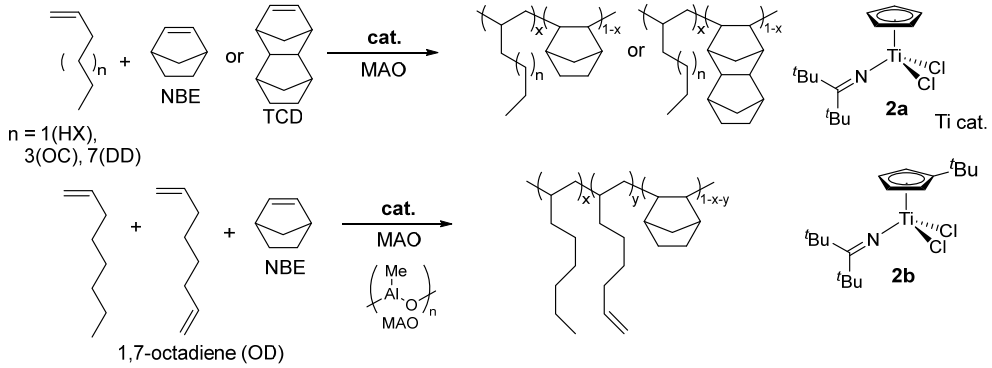

Scheme 6. Copolymerization of norbornene (NBE), tetracyclododecene (TCD) with α-olefin (1-hexene, 1-octene, 1-dodecene, 1,7-octadiene) [65].

3. Ethylene Copolymerization with Sterically Encumbered Olefins

Ethylene copolymerization with 1,1-disubstituted α-olefins such as isobutene (IB), 2-methyl-1-pentene (2M1P) has rarely been reported in metal-catalyzed olefin coordination insertion polymerization [115]; these monomers have long been regarded as "traditionally unreactive" in this field. However, these ethylene copolymers are expected to show enhanced weather resistance compared with conventional ethylene/α-olefin copolymers, because of absence of reactive tertiary C–H bonds in the polymer backbone, which are removed by oxidative or UV-induced degradation. For instance, the ethylene/IB copolymerization using [Et(indenyl)$_2$]ZrCl$_2$ gave the copolymer with low (<2.8 mol%) IB content even under large excess IB concentration conditions (charge molar ratio of ethylene/IB = 1/4000) [116].

Ordinary **CGC** showed the negligible IB incorporation in the ethylene copolymerization, the IB incorporation was much improved by using cyclododecylamide analogue (**CGC-CDD**, Scheme 7) [117]; the fluorenyl analogue (**Flu-CGC-CDD**, Scheme 7) later showed the IB incorporation [118]. However, the copolymerization with 2M1P by **CGC-CDD** afforded the polymer possessing large PDI (polydispersity index, M_w/M_n = 5.90) [117]. The **bimetallic CGC**, consisting of dinuclear catalyst and dianionic borate catalyst system (Scheme 7), showed improved IB incorporation from the mononuclear **CGC** (IB 3.1 mol% *vs* 15.2 mol%: ethylene 1 atm, IB 1.3 M, 24 ºC), but showed low activity decreased and the obtained polymer possessed rather large PDI (M_w/M_n = 3.67) [119,120]. The catalyst system incorporated methylenecyclopentene and methylenecyclohexene in the ethylene copolymerization. The attempted copolymerization with 2-methyl-2-butene gave the copolymer by incorporation as 2-methyl-1-butene formed by olefin isomerization [120]. Reports for synthesis of high molar mass ethylene copolymers with 1,1-disubstituted α-olefin (except IB) have still remained scarce.

Synthesis of ethylene/2M1P copolymers was achieved by the phenoxide modified half-titanocene catalyst with rather efficient 2M1P incorporation (**1a**, M_n = 3.30-13.0×10^4, M_w/M_n = 1.70-1.90) [71,73]. As summarized the selected data in Table 3, 2M1P content in the resultant copolymer increased upon increasing upon increase in the 2M1P concentration charged or lowering ethylene pressure (6 → 4 atm) with decrease in the activity [71,73]. The resultant copolymers possessed uniform compositions confirmed by DSC thermograms and their microstructural analysis by ^{13}C NMR spectra revealed that 2M1P was incorporated in an isolated and/or alternating manner (without repeat insertions). Use of the *tert*-BuC$_5$H$_4$ analogue (**1c**) led to decrease in both the activity and the

 doi:10.20944/preprints202601.2232.v1

2M1P incorporation explained as due to the steric bulk [71,73]. Later, the activity by the $SiEt_3$ analogue (**1b**) increased at elevated temperature (up to 80 ºC) [75]. In contrast, the Cp–ketimide analogue (**2a**) showed poor 2M1P incorporation, suggesting that nature of anionic donor ligand (as well as steric bulk on Cp′) affect the comonomer incorporation. Moreover, as described above, **CGC** also showed poor 2M1P incorporation under the same conditions.

The Cp*–phenoxide analogue (**1a**) also showed efficient VCH incorporation in the ethylene copolymerization [72], whereas incorporation of branched (γ-disubstituted) α-olefins in the copolymerization using the conventional catalysts seemed difficult [72]. However, as summarized in Table 3, **1a** showed negligible *tert*-butyl ethylene incorporation, and showed rather poor VTMS incorporation compared to the Cp–ketimide analogue (**2a**), **CGC**; the VTMS incorporation was improved by using the *tert*-BuC_5H_4 analogue (**1c**) but the resultant copolymer possessed rather low M_n values compared with those prepared by **2a** [121]. Synthesis of ethylene copolymers with *tert*-butyl ethylene (TBE) was achieved by the *tert*-BuC_5H_4 analogue (**1d**) and the 1,2,4-$Me_3C_5H_2$ analogue (**1e**); the observed effect on Cp′ was the same as that in the ethylene copolymerization with cyclohexane [68].

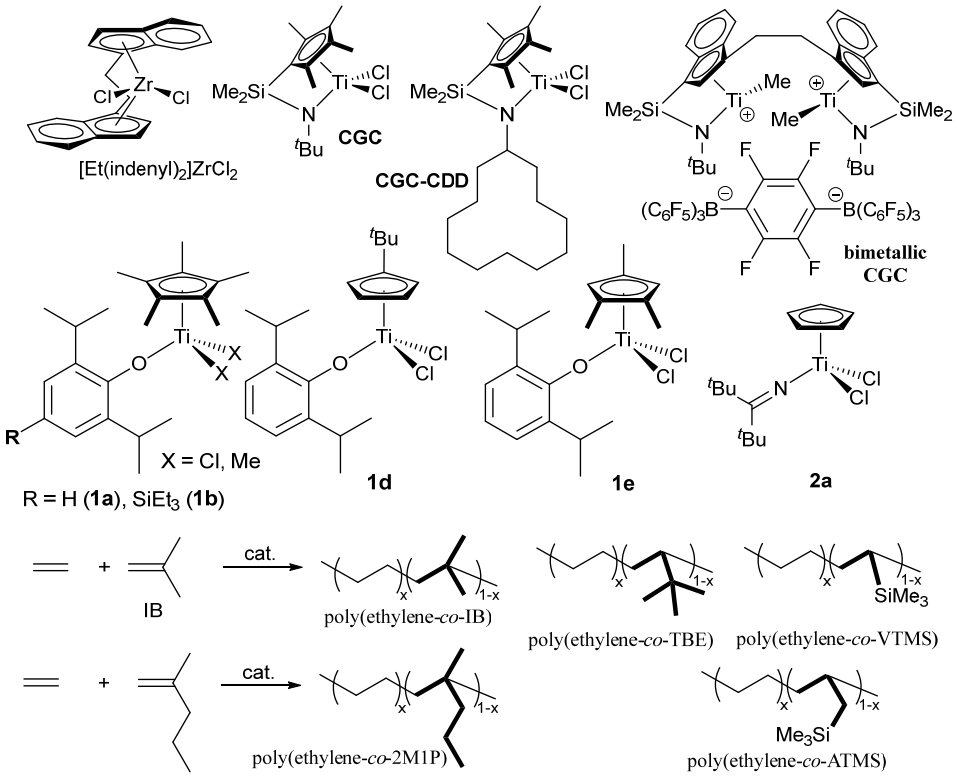

Scheme 7. Ethylene copolymerization with α-olefins containing steric bulk [71–75,116–121].

Table 3. Ethylene (E) copolymerization with 2-methyl-1-pentene (2M1P), *tert*-butylethylene (TBE), and with vinyltrimethylsilane (VTMS) by Cp′$TiCl_2$(OAr) [OAr = O-2,6-^{i}Pr$_2$C$_6$H$_3$, Cp′ = Cp* (**1a**), ^{t}BuC_5H_4 (**1d**)], $CpTiCl_2(N=C^tBu_2)$ (**2a**), $[Me_2Si(C_5Me_4)(N^tBu)]TiCl_2$ (**CGC**)–MAO catalysts (in toluene at 25 °C, 10 min).[a]

cat. (μmol)	E/ atm	comonomer/ M[b]		activity[c]	M_n[d]×10^{-4}	M_w/M_n[d]	cont.[e]/ mol%
1a (0.10)	4	---	-	12100	40.0	3.70	
1a (0.50)	6	2M1P	1.35	6980	13.0	1.70	
1a (0.50)[f]	6	2M1P	1.35	8460	12.0	2.10	3.3
1a (0.50)[f]	6	2M1P	2.70	5760	10.0	1.80	5.7
1a (0.50)[f]	4	2M1P	1.35	4240	6.50	2.00	5.0

 doi:10.20944/preprints202601.2232.v1

1a (0.50)[f]	4	2M1P	2.70	2680	4.90	1.60	9.4
1d (2.0)	6	2M1P	1.35	573	5.80	2.00	
2a (0.20)	6	2M1P	-	19100	53.0	2.10	
2a (0.20)	6	2M1P	1.35	10100	43.0	2.00	
2a (0.20)	6	2M1P	2.70	6960	34.0	1.80	0.3
CGC (1.0)[g]	6	2M1P	2.70	1840	12.0	2.40	0.3
CGC (1.0)[g]	4	2M1P	1.35	1420	9.70	2.50	
CGC (1.0)[g]	4	2M1P	2.70	1320	7.40	2.40	0.4
1a (0.20)	6	TBE	1.29	14100	15.5	2.00	trace
1a (0.50)	6	VTMS	1.15	1870	30.5	1.90	5.1
1d (1.0)	6	TBE	2.58	3310	11.7	2.50	1.3
1d (1.0)[h]	4	TBE	1.60	2020	8.17	2.40	3.3
1d (2.0)[h]	2	TBE	1.60	918	7.27	2.10	4.4
1d (2.0)[h]	2	TBE	3.90	756	4.04	2.00	6.8
1d (0.20)	6	VTMS	1.15	92	1.41	2.80	13.6
2a (0.20)	6	TBE	1.29	7830	71.1	1.90	trace
2a (0.20)	6	TBE	2.58	6000	68.7	1.90	trace
2a (1.0)	6	VTMS	1.15	3730	57.3	2.30	11.9
2a (1.0)	4	VTMS	1.15	1560	42.2	2.30	18.7
CGC (0.25)	6	TBE	1.29	3020	32.0	2.00	none
CGC (0.25)	6	VTMS	1.15	2280	36.7	2.50	10.4

[a]Conditions: Comonomer+toluene total 30 mL, d-MAO 3.0 mmol. [b]Initial comonomer feed conc. (mmol/mL). [c]Activity in kg-polymer/mol-Ti·h. [d]GPC data in *o*-dichlorobenzene *vs* PS stds. [e]Comonomer content (mol%) estimated by ^{13}C NMR spectra. [f]MAO 4.5 mmol. [g]Polymerization 6 min. [h]TBE+toluene total 10 mL.

– Effect of Borate Cocatalysts toward Activity, Comonomer Incorporation in Alkane Solvent –

Recently, it has been recognized that solvent coordination (toluene *vs* alkane) in addition to catalyst–cocatalyst interaction (nuclearity effect) affect both the catalytic activity, comonomer incorporation in olefin polymerization [75,122,123]. For instance, [Me$_2$Si(C$_5$Me$_4$)(N^{t}Bu)]TiCl$_2$ (**CGC**), Cp*TiMe$_2$(O-2,6-^{i}Pr$_2$-4-RC$_6$H$_2$) [R = H (**1a'**), SiEt$_3$ (**1b'**)]–borate, [A(H)]$^+$[BAr$_4$]$^-$ (Ar = C$_6$F$_5$ or C$_{10}$F$_7$, **B1**–**B6** in Scheme 8), catalyst systems conducted in methylcyclohexane (MCH) exhibited better comonomer incorporation than those conducted in toluene (in the presence of MAO, borate cocatalysts) in the ethylene copolymerization with 2M1P, 1-dodecene, VCH [75].

The activity by **CGC** in the E/2M1P (co)polymerization (ethylene 4 atm, 25 ºC) in MCH was affected by the borate cocatalyst employed and increased in the order: activity = 149 kg-polymer/mol-Ti·h (**B1**) < 768 (**B6**) < 2660 (**B5**) < 3770 (**B2**) < 6810 (**B3**). Interestingly, **CGC**–**B3** catalyst system in MCH afforded the copolymer (2M1P 0.4 mol%, by DSC thermogram and ^{13}C NMR spectrum), whereas **CGC**–MAO catalyst system in toluene showed negligible 2M1P incorporation under the same conditions [75]. It seems that the 2M1P incorporations (estimated by the T_m values) were also affected by the borate cocatalyst employed. Similarly, the activities by **1a'** and **1b'** were affected by the borate cocatalyst employed, and **1b'**–**B5** catalyst system showed the highest activity (5060 kg-polymer/mol-Ti·h) and the resultant copolymer possessed higher 2M1P content than that conducted in toluene by **1b'**–MAO catalyst system (6.0 mol% vs 3.1 mol%) [75]. In contrast, **1b'**–**B1** catalyst system showed low activity affording the polymer with two compositions estimated by DSC thermograms. It should be noted that the 2M1P incorporation was affected by the borate cocatalyst employed: **B5** showed better 2M1P incorporation than **B3**. It was shown that conducting these copolymerizations in MCH in the presence of borate cocatalysts (**B2**–**B6**) showed better 2M1P incorporation than that conducting in toluene in the presence of MAO [75].

 doi:10.20944/preprints202601.2232.v1

Moreover, the activity by **CGC** conducted in MCH was affected by the borate cocatalyst employed. **CGC**–**B5** catalyst system in MCH exhibited higher catalytic activity and better VCH incorporation than **CGC**–MAO catalyst system in toluene [75]. Note that no significant differences in the VCH contents in the copolymers were observed when these polymerizations using **CGC**–borate catalyst systems were conducted in toluene; the VCH incorporation was thus affected by the solvent (toluene *vs* MCH). The results thus suggest that the observed difference in MCH would be due to a weak cation–anion interaction *without* coordination of toluene (and amine or ether, exhibited A formed after treatment of **CGC** with borate) to the assumed cationic alkyl species [122–124]. Non-coordinating oxonium ion, especially $HO^+(n\text{-}C_{14}H_{29})_2{\cdot}O(n\text{-}C_{14}H_{29})_2$ (**B5**) containing long alkyl chains, was preferred than the ammonium salts (probably due to poor coordination ability of $O(n\text{-}C_{14}H_{29})_2$ to the assumed cationic species) [75]. As expected for better anion delocalization (BAr_4^-), perfluorinated naphthyl borate, $B(C_{10}F_7)_4^-$, showed higher activity than $B(C_6F_5)_4^-$.

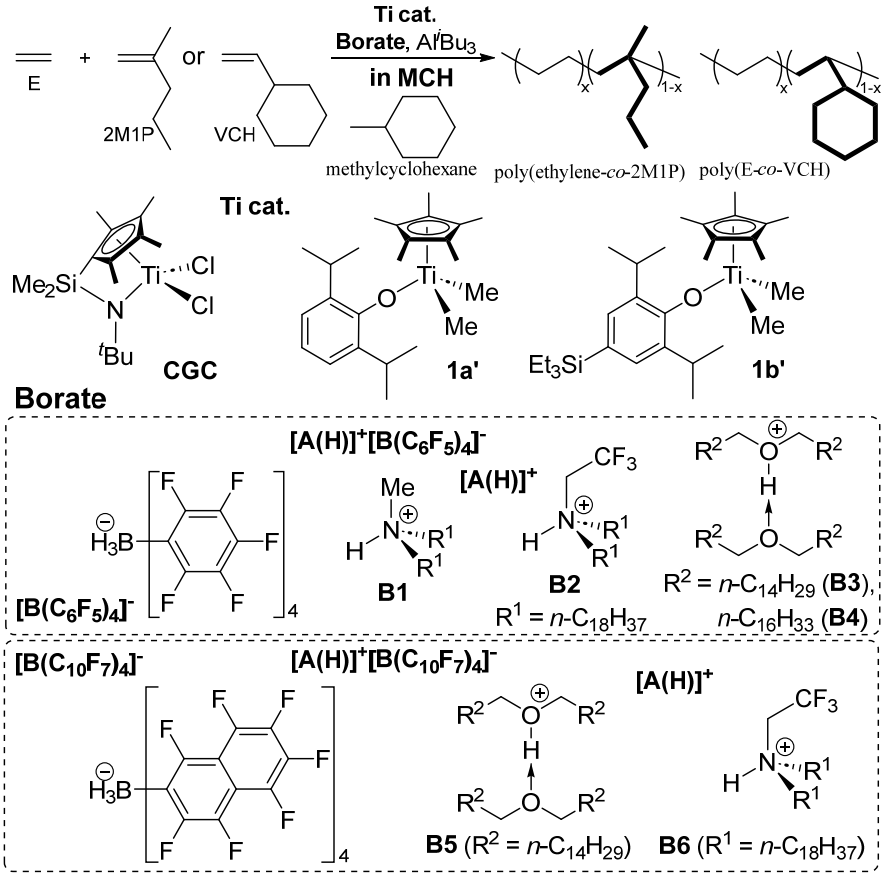

Scheme 8. Effect of borate cocatalysts (**B1**–**B6**) in Ethylene copolymerization with 2-methyl-1-pentene (2M1P), vinylcyclohexane (VCH) by $[Me_2Si(C_5Me_4)(N^tBu)]TiCl_2$ (**CGC**), $Cp^*TiMe_2(O\text{-}2,6\text{-}^iPr_2\text{-}4\text{-}R'C_6H_2)$ [R′ = H (**1a′**), $SiEt_3$ (**1b′**)] in methylcyclohexane (MCH) [75].

Table 4. Ethylene copolymerization with 2-methyl-1-pentene (2M1P) or vinylcyclohexane (VCH) by $[Me_2Si(C_5Me_4)(N^tBu)]TiCl_2$ (**CGC**), $Cp^*TiMe_2(O\text{-}2,6\text{-}^iPr_2\text{-}4\text{-}R'\text{-}C_6H_2)$ [R = H (**1a′**), $SiEt_3$ (**1b′**)]–borate cocatalyst systems [at 25 °C, ethylene 4 atm, 10 min (2M1P); ethylene 6 atm 6 min (VCH)].[a]

cat. (μmol)	solvent	Al cocat.	borate	comonomer	activity[b]	M_n[c] ×10⁻⁴	M_w/M_n[c]	T_m[d] / °C	cont.[e] / mol%
CGC (1.0)	MCH	Al^iBu_3[f]	**B1**	2M1P	149	6.88	3.09	131	
CGC (1.0)	MCH	Al^iBu_3[f]	**B2**	2M1P	3770	38.9	5.88	122	

 doi:10.20944/preprints202601.2232.v1

CGC (1.0)	MCH	Al^{i}Bu$_3$[f]	**B3**	2M1P	6810	44.9	6.42	120	0.4
CGC (1.0)	MCH	Al^{i}Bu$_3$[f]	**B5**	2M1P	2660	32.0	5.66	122	
CGC (1.0)	MCH	Al^{i}Bu$_3$[f]	**B6**	2M1P	768	26.1	5.23	126	
CGC (0.1)	toluene	MAO	---	2M1P	5090	32.4	3.66	129	trace
1a′ (1.0)	MCH	Al^{i}Bu$_3$	**B3**	2M1P	4210	6.28	1.93	99.0	5.5
1a′ (1.0)	MCH	Al^{i}Bu$_3$	**B4**	2M1P	1280	7.87	1.84	96.9, 122	
1a′ (1.0)	MCH	Al^{i}Bu$_3$	**B5**	2M1P	4260	5.76	1.76	93.6	6.8
1a′ (1.0)	MCH	Al^{i}Bu$_3$	**B6**	2M1P	1870	4.93	1.89	94.5	
1a′ (0.05)	toluene	MAO	---	2M1P	11200	8.41	2.25	111	2.6
1b′ (1.0)	MCH	Al^{i}Bu$_3$	**B1**	2M1P	547	7.04	2.47	99.5, 121	
1b′ (1.0)	MCH	Al^{i}Bu$_3$	**B2**	2M1P	2680	3.82	1.96	98.7	
1b′ (1.0)	MCH	Al^{i}Bu$_3$	**B3**	2M1P	4040	4.11	1.90	101	5.0
1b′ (1.0)	MCH	Al^{i}Bu$_3$	**B4**	2M1P	3980	3.21	2.41	98.4	
1b′ (1.0)	MCH	Al^{i}Bu$_3$	**B5**	2M1P	5060	5.41	1.84	97.9	6.0
1b′ (0.05)	toluene	MAO	---	2M1P	18600	8.34	2.05	109	3.1
CGC (0.05)	MCH	Al^{i}Bu$_3$	**B2**	VCH	16800	7.70	1.70	87.5	8.8
CGC (0.05)	MCH	Al^{i}Bu$_3$	**B3**	VCH	44000	6.31	1.65	86.0	9.0
CGC (0.05)	MCH	Al^{i}Bu$_3$	**B4**	VCH	10600	5.93	1.75	87.0	8.7
CGC (0.05)	MCH	Al^{i}Bu$_3$	**B5**	VCH	69000	8.65	1.98	81.4	9.7
CGC (0.05)	toluene	MAO	---	VCH	39400	21.4	3.38	92.5	6.0
CGC (0.05)	toluene	Al^{i}Bu$_3$	**B1**	VCH	1090	10.8	2.28	98.6	
CGC (0.05)	toluene	Al^{i}Bu$_3$	**B2**	VCH	16500	13.0	2.30	96.3	5.6
CGC (0.05)	toluene	Al^{i}Bu$_3$	**B3**	VCH	14100	13.1	2.59	96.9	5.6
CGC (0.05)	toluene	Al^{i}Bu$_3$	**B4**	VCH	21100	8.55	2.21	97.0	5.4
CGC (0.05)	toluene	Al^{i}Bu$_3$	**B5**	VCH	31000	13.8	3.07	94.2	5.8
1b′ (0.01)	toluene	MAO	---	VCH	224000	17.5	2.43	(-15.1)	24.1

[a]Conditions: 2-Methyl-1-pentene (2M1P) 5.0 mL (1.35 M) or vinylcyclohexane (VCH) 5.0 mL (1.22 M), 2M1P (or VCH) + methylcyclohexane (MCH) or toluene total 30.0 mL, Al^{i}Bu$_3$ [0.55 mmol/L hexane, Al/Ti = 1000 (molar ratio)] or MAO 3.0 mmol, borate (borate/Ti molar ratio = 1.0). [b]Activity = kg-polymer/mol-Ti·h. [c]GPC data in *o*-dichlorobenzene *vs* polystyrene standards (M_n in g/mol). [d]By DSC thermograms. [e]2M1P or VCH content (mol%) estimated by ^{13}C NMR spectra. [f]Al/Ti = 500, molar ratio.

4. Synthesis of Biobased Polyolefins: Copolymerization of Biobased Conjugated Dienes

Development of functional polymers from renewable feedstocks has been an important subject in circular economy [125–132]. Cyclic monoterpenes consisting of two isoprene units as formula of $C_{10}H_{16}$ shown in Scheme 9, can be considered as promising monomers obtained from the abundant plant oil [133,134]. However, the successful synthesis by coordination insertion polymerization has been scarce until recently [69,135], whereas there are the reports by ionic (cationic, radical) polymerization.

(1,2,4-Me$_3$C$_5$H$_2$)TiCl$_2$(O-2,6-^{i}Pr$_2$C$_6$H$_3$) (**1e**) enabled synthesis of ethylene/limonene copolymers possessing rather high molecular weights (M_n = 4.00-12.6×10^4) with unimodal molecular weight distributions [135]. As observed in the ethylene/2M1P copolymerization (Table 3), increase in the limonene concentration led to decrease in the activity and the M_n value in the copolymer, while simultaneously increasing the limonene content in the copolymer. In contrast, the Cp* analogues (**1a**,**b**) showed less efficient limonene incorporation and **CGC** showed the negligible incorporation.

 doi:10.20944/preprints202601.2232.v1

Microstructural analysis revealed resonances consistent with 1,2-limonene insertion followed by cyclization, favoring a 2′,1′-insertion (than 1′,2′-insertion) pathway (Scheme 9) [135].

The Cp* analogues (**1a**,**b**)–MAO catalyst gave high molar mass poly(ethylene-*co*-*β*-pinene)s (M_n = 2.10-22.4×10⁴) possessing unimodal molecular weight distributions (M_w/M_n = 1.53-2.32). The activity was influenced by the *β*-pinene concentration charged, ethylene pressure, Al/Ti molar ratio and the temperature. The 1,2,4-$Me_3C_5H_2$ analogue (**1e**) showed the low activities compared with **1a**,**b**, affording the copolymers possessing rather low M_n values [135]. The attempted copolymerization by **CGC** gave polymers with negligible *β*-pinene incorporation.

β-Myrcene (myrcene, My), a promising biobased linear terpene, has been polymerized by radical or anionic polymerization and reports concerning the metal catalyzed ethylene copolymerization have been limited by scandium catalysts [136] or half-titanocene catalysts [69], whereas there are reports for the styrene/My copolymerization [137–143]. The scandium catalysts, however, afforded copolymers possessing multi-block microstructures, expressed as poly(E-*bl*-My), possessing melting temperature of polyethylene segment (133 ºC, My 9 mol%) [136]. Phenoxide-modified Cp* analogues (**1a**,**b**) demonstrated synthesis of high molar mass (semicrystalline or amorphous) random ethylene/My copolymers with efficient My incorporation [69]. The microstructural analysis using ^{13}C NMR spectra of the resultant (unsaturated) copolymers and the saturated copolymers prepared by olefin hydrogenation. The analysis data revealed that the copolymers possessed cyclopentane units containing My pendant arm (-CH_2CH=CMe_2); which are presumably formed by 2,1- or 1,4-My insertion and subsequent cyclization after ethylene insertion (Scheme 9) [69]. In general, formation of η^3-allyl intermediate, considered as dormant, disturbs proceeding further olefin insertion. In this catalysis, the subsequent cyclization enabled to proceed the copolymerization with random My incorporation. The elongation (tensile strain) at break increased with increasing the My contents accompanied with decrease in the tensile stress (strength); the copolymer showed promising elastic behaviors as biobased elastomers [69]. The catalysts also enabled synthesis of ethylene/isoprene copolymers possessing cyclopentane and cyclohexane units [70].

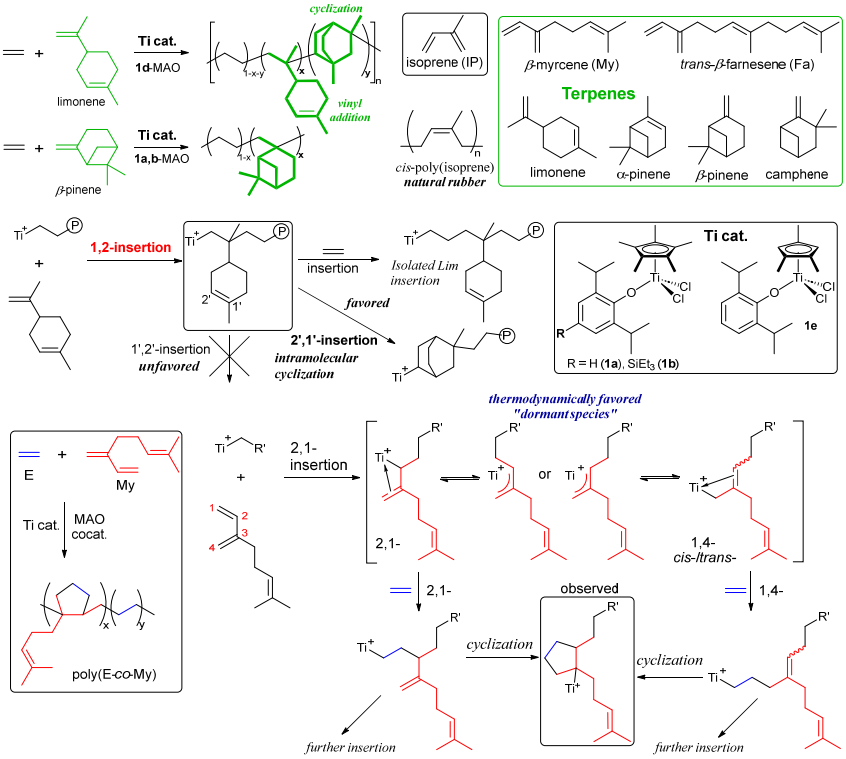

Scheme 9. Synthesis of biobased ethylene copolymers with limonene, *β*-pinene, and myrcene [69].

 doi:10.20944/preprints202601.2232.v1

5. Analysis of Catalytically Active Species Through XAS (X-Ray Absorption Spectra)

5.1. Introduction: XAS for Analysis of Catalytically Active Species

Identification of catalytically active species and the reaction chemistry are prerequisite not only for clear understanding the catalysis mechanism, but also for catalyst design through the structural and electronic insight. Single crystal X-ray diffraction analysis provides a structural information of the proposed intermediate(s) in solid state, although such species are often (sometimes) required by certain stabilization for isolation and the information is limited to be in solid state. Mechanistic studies are also supported by reaction chemistry, stoichiometric and/or catalytic reactions, using model complexes (and the isolated species in the catalytic reaction) and computational studies. However, we often observed that the isolated species exhibit apparently low catalytic activities or are inactive, due to required stabilization for the isolation and/or isolated species are indeed dormant in the catalysis cycle.

Nuclear magnetic resonance (NMR) spectroscopy is the principal technique for characterization of diamagnetic inorganic and organometallic compounds in (partially) deuterated solvent. Electron spin resonance (ESR) spectroscopy has been powerful method for analysis of the paramagnetic species that exhibit negligible or broadened NMR signals [144,145]. However, these methods still provide limited access for obtainment of real/clear structural information (image) in catalysis solution. Moreover, ESR often lacks quantitative analysis/reliability [144–146], and a possibility of co-presence of "ESR silent" species cannot be excluded. For example, vanadium(III) species with $3d^2$ electron configuration (S = 1, triplet, S = spin quantum number) are ESR silent due to an interaction between the two unpaired electrons, while vanadium(IV) dimers coupled antiferromagnetically also become ESR-silent through spin-orbit coupling (SOC) [146,147].

Analysis by XAS (X-ray absorption spectroscopy), XANES (XANES = X-ray Absorption Near Edge Structure) and EXAFS (EXAFS = Extended X-ray Absorption Fine Structure), performed at synchrotron facilities provides information of not only oxidation state and the basic geometry around the metal centre (by XANES), but also kind of atoms and the distances connected (coordinated) to the metal centre (by EXAFS). More recently, we see growth of number of reports identifying homogeneous, molecular catalysis through XAS analysis [27,76,148–159], whereas the methods are common in heterogeneous catalysis [160–164]. The methods are recognized as a useful analysis method especially of catalysis research with early transition metals, as exemplified in analysis of paramagnetic vanadium(III) species and titanium(III) species that cannot be observed especially by NMR spectroscopy [27,76,148,149,153,154,158].

Although we need to use the appropriate synchrotron facility (e.g. SPring-8, BL01B1 beamline), we do not need any specified apparatus, and the sample preparations are possible on site in the drybox. Moreover, we demonstrated good reproducibility (in the independent runs even conducted during the different beam time) and no severe x-ray radiation damages during data acquisition were observed [27,76]. Herein, we first describe basics in XAS analysis for uninitiated researchers and introduce selected results in analysis of catalytically active species in olefin polymerization and syndiospecific styrene polymerization using half-titanocene catalysts.

5.2. Basics in XANES Spectra

It has been known that pre-edge peak intensity and edge absorption (exemplified in Figure 1) in XANES spectra are influenced by the oxidation state and the basic geometry around the centred metal [27,148,149,160–173]. For basic introductory, V-K edge XANES spectra of vanadium oxides with various oxidation states are shown in Figure 1a [174]. The basic geometries [octahedral (O_h), square pyramidal (C_{4v})], tetrahedral (T_d)] and their selected irreducible and relating functions and point groups are also placed in the figure. Pre-edge absorption is known to provide information about basic (local) geometry around the metal center reflected by s → d transitions (quadrupole transition);

 doi:10.20944/preprints202601.2232.v1

dipole transition (s → p) is also considered depending on degree of p–d orbital hybridization [166,169,175,176]. For instance, complexes with T_d and C_{4v} symmetries display higher pre-edge peak intensity than those in O_h symmetry. The observed difference can be explained as due to a difference in the possibility of a p–d orbital hybridization, realized from a table in irreducible representations and the relating functions in the complexes with these symmetries (Figure 1b).

The complex with tetrahedral geometry (T_d) leads to increase degree of electric dipole transition of a 1s electron to the p–d hybridized orbital [166,169,175,176]. This is because that p_x, p_y, p_z orbitals and d_{xy}, d_{yz}, d_{zx} orbitals in T_d symmetry (or p_x, p_y orbitals and d_{yz}, d_{zx} orbitals in C_{4v} symmetry) belong to the irreducible representation, leading to formation of a p–d hybridized orbital with increased electric dipole transition of a 1s electron occurs to the hybridized orbital [169,176]. However, no irreducible representations containing d and p orbitals are present for the complexes with octahedral geometry (O_h point group). Therefore, the intensity of the pre-edge peak is generally weak, because only the relatively weak quadrupole transition (s → d transitions) is allowed, while the dipole transition (s → p) is forbidden; distortion of the symmetry (symmetry breaking), however, enables p–d hybridization that allows the dipole transition. Therefore, simple prediction of the pre-edge peak intensity could be possible without theoretical calculations by using the character tables of group theory. V_2O_3 and V_2O_4 also fold a distorted octahedral geometry fold a distorted octahedral geometry around vanadium, whereas V^{5+} ions in V_2O_5 fold distorted tetragonal pyramid [27,148,149,174]. Observed pre-edge peaks [at 5468.4 and 5469.8 eV (V_2O_3), 5470.0 eV (VO_2), 5470.8 eV in V_2O_5] are, as described above, generally assigned as due to a transition from 1s to 3d + 4p [166,169,175,176].

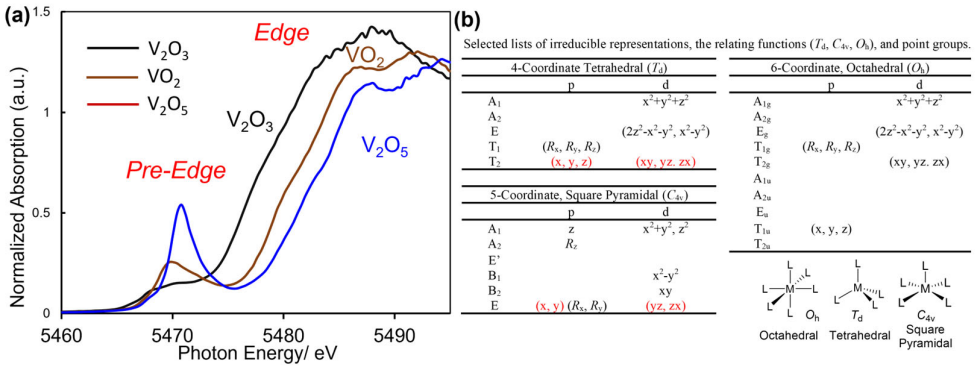

Figure 1. (a) V K-edge spectra (5.46 keV, by using synchrotron radiation at SPring-8, BL01B1 beamline) for vanadium oxides with various oxidation state, (b) selected irreducible and relating functions and point groups in octahedral, square pyramidal and tetrahedral complexes [27,148].

Figure 2a shows Ti K-edge XANES spectra in toluene for $CpTiCl_3$, Cp^*TiX_3 (X = OCH_3, Cl) measured at 25 ºC (Ti K-edge 4.97 keV, through use of synchrotron radiation at SPring-8, BL01B1 beamline). These spectra show rather strong pre-edge absorption at 4965-4967 eV due to tetrahedral geometry around titanium, as described above. Rather strong absorption bands called shoulder-edge at 4977.0 eV in Cp^*TiCl_3 and $CpTiCl_3$, whereas no such absorption was seen in $Cp^*Ti(OCH_3)_3$; the absorption was due to presence of Ti–Cl bond, known as a shakedown peak assigned to the metal 1s to 4p coupled with the ligand to metal charge transfer (LMCT) [170–173]. No significant differences in the spectra were seen between $CpTiCl_3$ and Cp^*TiCl_3, because of the similar geometry and number of chloride ligands around titanium.

Figure 2b shows Ti K-edge XANES spectra in toluene solution (at 25 °C, conc. 50 μmol-Ti/mL) for $Cp'TiCl_2(O\text{-}2,6\text{-}{}^iPr_2C_6H_3)$ [Cp' = Cp, $^tBuC_5H_4$ (**1d**), Cp* (**1a**)], $CpTiCl_2(N{=}C^tBu_2)$ (**2a**), and $[Me_2Si(C_5Me_4)(N^tBu)]TiCl_2$ (**CGC**) [27]. The XANES spectrum of **1a** shows strong pre-edge absorptions at 4966.2 and 4967.6 eV and these are similar to those in the dimethyl complex, $Cp'TiMe_2(O\text{-}2,6\text{-}{}^iPr_2C_6H_3)$ (**1a'**), which showed at 4966.1 and 4967.7 eV. As described above, these

 doi:10.20944/preprints202601.2232.v1

are generally considered as due to a transition from 1s to 3d + 4p [166,169,175,176]. Moreover, as described above, **1a** shows an absorption maxima at 4978.0 eV (called as shoulder-edge) ascribed to a presence of Ti–Cl bond [76,170–173]. Interestingly, as described above, positions of the edge peak (absorption) and the intensities in the half-titanocenes chosen in Figure 2b are close, whereas **CGC** shows rather high intensity at the pre-edge absorption at 4967.6 eV. Moreover, the spectra in toluene solution were highly analogous to those measured in solid (tablets with boron nitride) [76], strongly suggesting that these are Ti(IV) complexes with (a distorted) tetrahedral geometry in solid and solution [76].

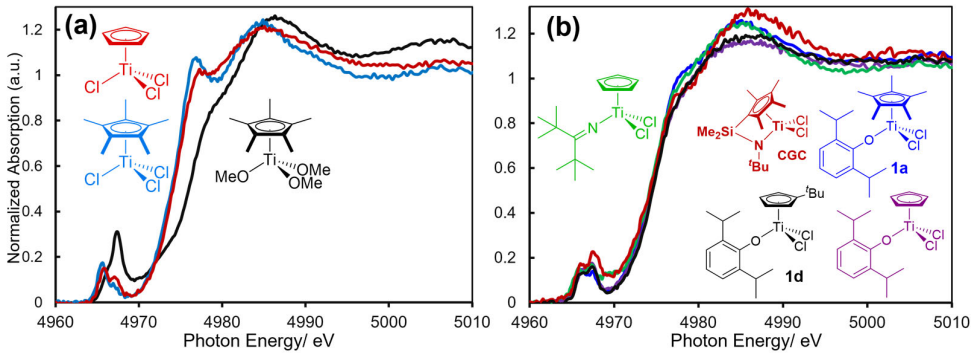

Figure 2. The solution-phase Ti K-edge XANES spectra (in toluene at 25 ºC, Ti K-edge 4.97 keV, through the use of synchrotron radiation at SPring-8, BL01B1 beamline) for (a) $CpTiCl_3$, Cp^*TiX_3 (X = OCH_3, Cl), and (b) $Cp'TiCl_2(O\text{-}2,6\text{-}{}^iPr_2C_6H_3)$ [Cp' = Cp, $^tBuC_5H_4$ (**1d**), Cp^* (**1a**)], $CpTiCl_2(N{=}C^tBu_2)$ (**2a**), and $[Me_2Si(C_5Me_4)(N^tBu)]TiCl_2$ (**CGC**) [27,76].

5.3. XAS Analysis for Exploring Active Species in Olefin Polymerization and Syndiospecific Styrene Polymerization by Half-Titanocene Catalysts

The high oxidation state group 4 cationic metal-alkyl species, Cp'_2M^+R (R = alkyl) or $Cp'M^+(Y)R$ (Y = anionic ancillary donor), formed from the dialkyl analogues by reaction with borate or MAO through alkyl abstraction, play an essential role as the catalytically active species in this catalysis cycle (Scheme 10) [5,9–17,24–27]. However, effective catalysts for olefin polymerization (especially metallocene, linked-half-titanocene) display poor (negligible) capability for synthesis of syndiotactic polystyrene (SPS) [34,36–39]. In contrast, half-titanocene catalysts, $Cp'TiX_3$ (X = F, Cl, OMe etc.), enables high catalytic activities for syndiospecific styrene polymerization (SSP) [38–40], whereas these catalysts exhibited low catalytic activities for ethylene polymerization and afforded a mixture of polyethylene, SPS and the copolymer, poly(ethylene-*co*-styrene) [34,41]. It has thus been recognized that the active species between olefin polymerization and SSP are different. The oxidation state of the active species in the SSP had thus been proposed as cationic Ti(III) species [177–179] or neutral Ti(III) species [56,57,180,181]. However, these mechanistic studies lacked "direct evidence" until recently, especially from the catalyst solution in the presence of styrene and MAO.

As described above, XANES (XANES = X-ray Absorption Near Edge Structure) and EXAFS (EXAFS = Extended X-ray Absorption Fine Structure) analyses provide direct information of not only oxidation state and the basic geometry around the metal centre (by XANES), but also kind of atoms and the distances connected (coordinated) to the metal centre (by EXAFS). Therefore, here introduces summary of the mechanistic studies reported recently [27,76].

 doi:10.20944/preprints202601.2232.v1

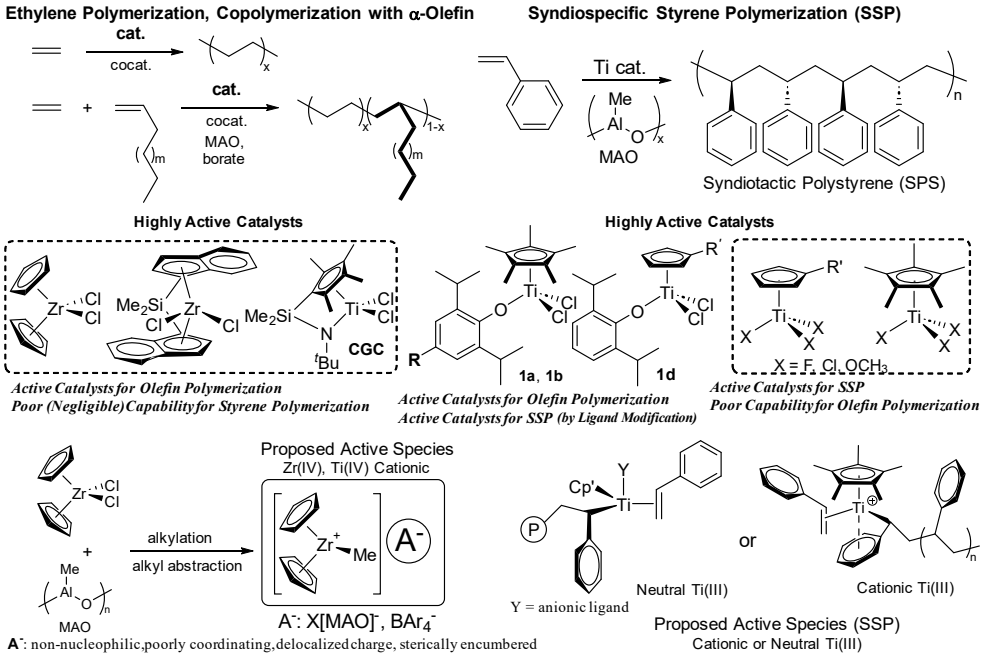

Scheme 10. Proposed catalytically active species in olefin polymerization and syndiospecific styrene polymerisation (SSP).

Figure 3a shows the XANES spectra for the phenoxide-modified half-titanocene dichloride (**1a**) and dimethyl complexes (**1a'**), and the catalyst solution in the presence of MAO and 1-hexene, exhibiting catalytic activities for 1-hexene polymerisation *in situ* [27,76]. These complexes (**1a**,**1a'**) exhibit high catalytic activities for ethylene polymerization [14–17,42–44], α-olefin polymerization [182], and ethylene copolymerization with various monomers (as described above) [14–17,42–44].

As shown in Figure 3a, the pre-edge peak positions and edge absorption of **1a** [4966.2 and 4967.6 eV (pre-edge), 4978.0 eV (shoulder-edge)] did not change upon addition of MAO, whereas intensity in the shoulder edge absorption in **1a**, ascribed to Ti–Cl bond, decreased upon addition of MAO (especially 50 equiv) [76]. No apparent changes in the spectra were observed even upon addition of excess 1-hexene (200 equiv). Moreover, the spectra did not change when the dimethyl complex (**1a'**) was added MAO (10 equiv). These results strongly suggest that the oxidation state as well as basic geometry around titanium preserved under these conditions even addition of MAO and 1-hexene (excess amounts). Similarly, as shown in Figure 3b, no significant differences in the XANES spectra were seen when the **1d** was treated with d-MAO and 1-hexene [76]. These results also suggest the same possibility that major species formed as Ti(IV) species upon addition of MAO.

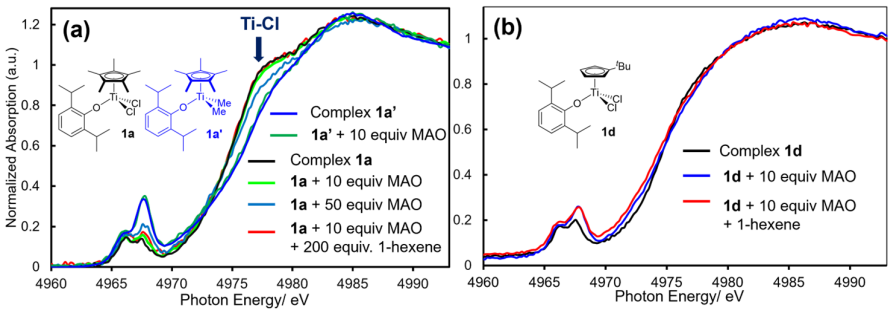

Figure 3. Ti K-edge XANES spectra (in toluene at 25 ºC) for (a) Cp*TiX$_2$(O-2,6-^{i}Pr$_2$C$_6$H$_3$) [X = Cl (**1a**), Me (**1a'**)] or (b) (^{t}BuC$_5$H$_4$)TiCl$_2$(O-2,6-^{i}Pr$_2$C$_6$H$_3$) (**1d**), and the spectra upon addition of MAO, and 1-hexene [76].

 doi:10.20944/preprints202601.2232.v1

Although no significant changes in the XANES spectra were observed, the corresponding EXAFS spectra, shown in Figure 4 [oscillations (left) and the FT-EXAFS spectra (right)], provide the clearer image, information in the reactions. The XANES spectra for Cp*TiCl$_2$(OAr) (**1a**) and the catalyst solution in the presence of MAO (10 and 50 equiv) showed no distinct spectral changes in toluene solution and in solid state (in solid, disk with boron nitride) measured at 25 °C (Figures 4a,b). The summary of coordination number (C.N.) and the distance (Å) in the atoms connected to titanium analyzed through the curve-fitting are summarized in Table 5 [76].

The Ti–C (on Cp′ coordinated) and Ti–O (phenoxide) bonds were preserved even after treating **1a** with MAO (10 and 50 equiv). In contrast, C.N. of Ti–Cl decreased by treating with MAO (Figure 4d, Table 5), clearly indicating that the Ti–Cl bonds were reacted (dissociated) with MAO (alkylation). Since separation of Ti–C and Ti–O bond seemed difficult (distances are close) in the analysis, observed increase in the C.N. of Ti–O bond upon addition of MAO could be explained as due to a subsequent formation of Ti–C bond [76]. These data also suggest that the Ti–Cl bonds in **1a** was reacted with MAO without dissociation of the Ti–O bond to form dimethyl complexes; the data support that the Ti(IV)-alkyl species play a role in this catalysis [14–17,76].

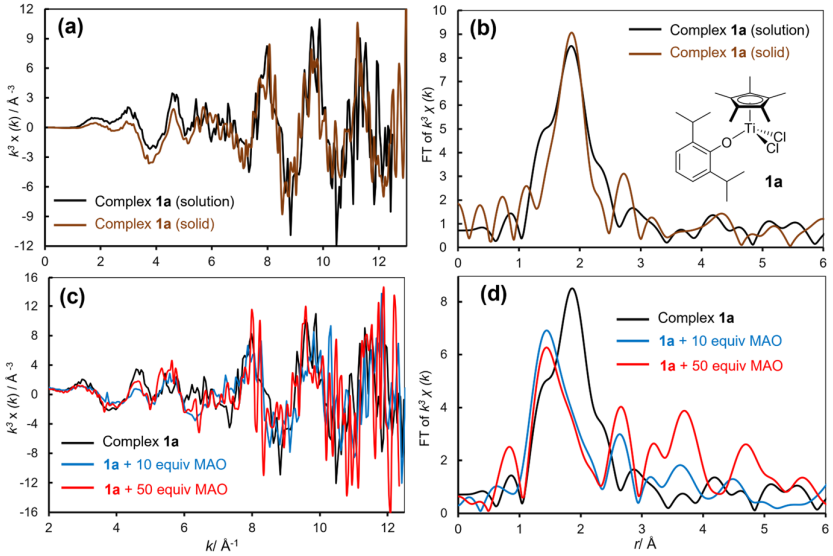

Figure 4. Ti K-edge (a) EXAFS oscillations and (b) FT-EXAFS spectra (in toluene at 25 ºC) for Cp*TiCl$_2$(OAr) (**1a**) by treating with MAO (10 or 50 equiv) [76].

Table 5. Summary of analysis data (by curve fitting) for toluene solution of Cp*TiCl$_2$(O-2,6-^{i}Pr$_2$C$_6$H$_3$) (**1a**), and **1a** treated with MAO (10 and 50 equiv) [76].

atom[a]	Cp*TiCl$_2$(OAr) (**1a**)			**1a** + 10 equiv MAO[e]			**1a** + 50 equiv MAO[e]		
	C.N.[b]	*r* (Å)[c]	D.W.[d]	C.N.[b]	*r* (Å)[c]	D.W.[d]	C.N.[b]	*r* (Å)[c]	D.W.[d]
O	1.3(1)	1.803(6)	0.0013(10)	2.3(2)	1.81(1)	0.0035 (12)	3.4(6)	1.87(1)	0.0059(25)
C	4.7(9)	2.42(1)	0.0030(19)	5.5(9)	2.13(2)	0.0047(22)	4.5(9)	2.14(1)	0.0040(30)
Cl	2.4(3)	2.269(7)	0.0047(13)	0.9(3)	2.18(3)	0.0062(49)			

[a]Atom: Neighbor atom. [b]C.N.: coordination number. [c]*r*: bond length. [d]D.W.: Debye-Waller factor. [e]For analysis, fixed ΔE values were used. *R* factors = 11.4%, 14.8%, and 12.9%, respectively, for complex **1a**, **1a** treated with MAO (10 equiv, 50 equiv).

As described above, the oxidation state of the active species in the SSP has been proposed as cationic or neutral Ti(III) species, Cp′Ti$^+$(R)(styrene) [177–179] or Cp′Ti(R)(Y)(styrene) [56,57,180,181] (Scheme 10). The cationic Ti(III) species were proposed based on the results in ESR measurement [177], reaction chemistry (formation of SPS) [179], and theoretical support [178]. The neutral Ti(III)

 doi:10.20944/preprints202601.2232.v1

species were proposed based on the results of (i) polymerization data (ligand effect, anionic donor) [56,57], (ii) step (co)polymerization [181], and (iii) theoretical support [180]. However, until recently, there were no "direct evidence" from the catalyst solution containing MAO and styrene [27,76,183].

Figure 5 shows Ti K-edge XANES spectra (in toluene at 25 ºC) for Cp'TiCl$_2$(OAr) [Cp' = ^{t}BuC$_5$H$_4$ (**1d**, left), Cp (**1e**, right)], and the spectra of solutions containing **1d** or **1e** and MAO (50 equiv), styrene (200 equv), which produce SPS *in situ*. The XANES spectrum of **1d** shows pre-edge absorptions (4966.5, 4967.5 eV) and a shoulder-edge absorption (4977.9 eV, presence of Ti–Cl bond) [27,170–173]. Addition of MAO (50 equiv) did not lead the significant spectral changes except decrease in the intensity of the shoulder-edge absorption in **1d** was observed, suggesting dissociation of Ti–Cl bond by alkylation.[76]

In contrast, noteworthy, styrene addition (200 equiv) into the solution (**1d** and MAO 50 equiv) led to the clear low energy shift (2.2 eV on the basis of the inflection point) in the edge absorption accompanied with decrease in intensities of two pre-edge peaks. The results thus strongly suggest that complex **1d** was reduced by addition of styrene (not by MAO). Moreover, the low energy shift in the edge absorption was observed upon increase amount of styrene charged (100→200 equiv) [76]. Moreover, as shown in Figure 5b, the solution containing **1e** showed the similar change when 200 equiv of styrene and 50 equiv of MAO were added into a toluene solution, which also produce SPS *in situ* [57]. These analysis data strongly suggest a formation of Ti(III) species from Ti(IV), derived from **1d**, accompanied with the structural changes upon addition of styrene.

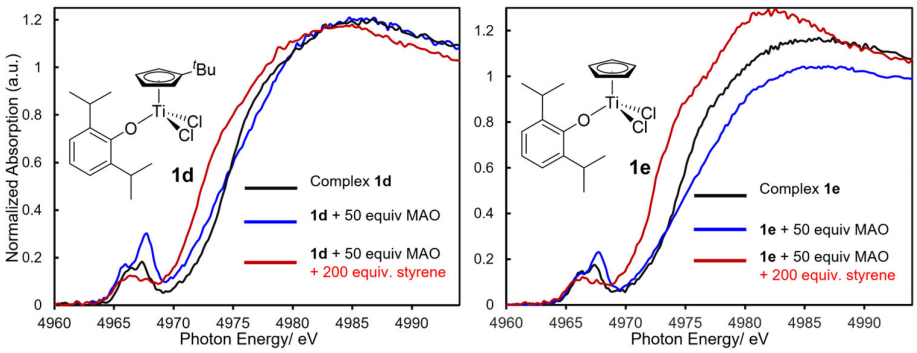

Figure 5. Ti K-edge XANES spectra (in toluene at 25 ºC) for Cp'TiCl$_2$(O-2,6-^{i}Pr$_2$C$_6$H$_3$) [Cp' = ^{t}BuC$_5$H$_4$ (**1d**), Cp (**1e**)], and the spectra for the catalyst solutions with addition of MAO, styrene [76].

Figure 6 shows EXAFS oscillations and the FT-EXAFS spectra (in toluene at 25 ºC) for (^{t}BuC$_5$H$_4$)TiCl$_2$(OAr) (**1d**), and the catalyst solution in the presence of MAO (50 equiv) and styrene (200 equiv), which showed the significant changes in the oxidation state upon addition of styrene in the XANES spectra (Figure 5). The analysis data by curve fitting are summarized in Table 6 [76].

Apparent change in the EXAFS oscillations from a toluene solution of **1d** to the solution with addition of MAO and styrene strongly suggest certain structural change (accompanied with change in the oxidation state). As observed by **1a**, C.N. of Ti–Cl diminished along with observation of new Ti–C bond which is formed by methylation with MAO, whereas C.N. and bond lengths in Ti–C bonds corresponding to Cp' were unchanged before/after the reaction. Importantly, preservation of the Ti–O bond (corresponding to phenoxide ligand) was confirmed even after **1d** was treated with MAO upon addition of styrene (200 equiv). The analysis data clearly demonstrate formation of the catalytically active species for SSP without dissociation of the Ti–O bond accompanied with reduction; the results thus strongly suggest an existence of the phenoxide species, (^{t}BuC$_5$H$_4$)Ti(R)(OAr) [or CpTi(R)(OAr)], in the solution [27,76]. The result is a good agreement with our previous assumption on the basis of two step ethylene/styrene (co)polymerization (Scheme 11) [181] as well as effect of anionic donor ligand in SSP [57] that the neutral Ti(III) species containing phenoxide ligand thus play a role for the SSP [181].

 doi:10.20944/preprints202601.2232.v1

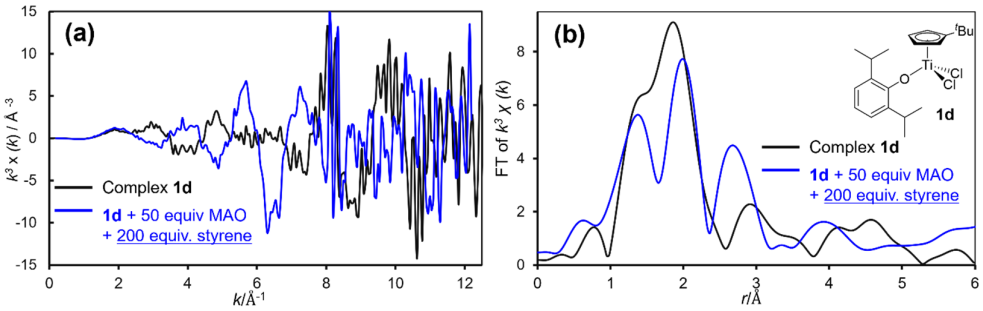

Figure 6. Ti K-edge (in toluene at 25 ºC) (a) EXAFS oscillations and (b) FT-EXAFS spectra for (^{t}BuC$_5$H$_4$)TiCl$_2$(OAr) (**1d**) upon addition of MAO (50 equiv) and styrene (200 equiv) [76].

Table 6. Summary of analysis data (by curve fitting) for toluene solution of (^{t}BuC$_5$H$_4$)TiCl$_2$(O-2,6-^{i}Pr$_2$C$_6$H$_3$) (**1d**), and **1d** with addition of MAO (50 equiv) and styrene (200 equiv) at 25 °C [76].

atom[a]	(^{t}BuC$_5$H$_4$)TiCl$_2$(OAr)[e] (**1d**)			**1d** + 50 equiv MAO + 200 equiv styrene[e]		
	C.N.[b]	r (Å)[c]	D.W.[d]	C.N.[b]	r (Å)[c]	D.W.[d]
O	1.3(1)	1.76(1)	0.0010(5)	0.7(4)	1.80(2)	0.0064(54)
Cl	1.7(1)	2.25(1)	0.0012(4)	---	---	---
C1	5.2(9)	2.41(2)	0.0055(45)	5.2(3)	2.40(1)	0.0040(15)
C2	---	---	---	1.3(6)	1.95(3)	0.0034(28)

[a]Atom: neighbor atom. [b]C.N.: coordination number. [c]r: bond length. [d]D.W.: Debye-Waller factor. [e]For analysis, fixed ΔE values were used. R factors = 10.7%, 7.5%, respectively, for complex **1d**, **1d** treated with MAO and styrene.

Moreover, the proposed catalytically active species based on XAS analysis as well as step ethylene/styrene (co)polymerization (Scheme 11a) was further supported by theoretical calculation [27,76,183]. DFT calculation was conducted for syndiospecific styrene insertion step of the three possible models of the active species containing the phenoxide ligand, neutral Ti(III), cationic Ti(IV), and Ti(IV)–B(C$_6$F$_5$)$_4$ catalysts (shown in Scheme 11b). The calculation was conducted from the Ti catalysts containing the phenylpropyl group, as a model of polystyrene in chain-propagation step (**R**; styrene + Ti, zero), and the styrene coordinated models (**IM**), and inserted model (**P**) in which styrene was inserted to the phenylpropyl moiety [76]. As shown in Scheme 11b, the results clearly indicate that the neutral Ti(III) catalyst exhibits the lower activation energy than the others, thus strongly support the above mechanism. The computational analysis also led to a conclusion that the neutral Ti(III) species containing the phenoxide ligand is more efficient and plausible catalyst model; formation of the Ti(III) species, proposed in Scheme 11, is a key to promote the SSP in an efficient manner [76]. Further DFT calculation results revealed that the neutral Ti(III) active species has high selectivity in SSP; the orientation of styrene (*si-*/*h-*/*re-*)insertions related to the stereoselectivity of polystyrene. The spin density analysis indicated the neutral Ti(III) center promote an electron transfer from the polymeric chain to the incoming styrene [183].

 doi:10.20944/preprints202601.2232.v1

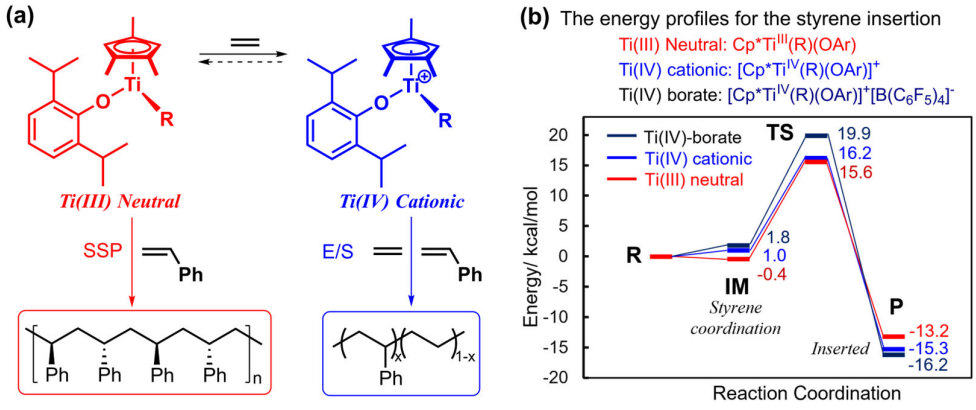

Scheme 11. (a) Proposed active species for syndiospecific styrene polymerization (SSP) confirmed by two step copolymerization, XAS analysis [76,181]. (b) The energy profiles for styrene insertion to assumed three species containing phenoxide ligand [76].

6. Concluding Remarks and Outlook

Olefin polymerization by group 4 transition metal catalysts has been the key technology for production of polyolefins, commodity plastics in our daily life. Development of new polymers, that cannot be achieved by using conventional catalysts has been the central research objective and copolymerization is an effective strategy. In this reviewing article, modified half-titanocenes, $Cp'TiX_2(Y)$ (Y = anionic donor such as phenoxide, ketimide, amidinate etc.) [6,14–17], contributed a significant effort for efficient, exclusive synthesis of ethylene copolymers containing cyclic olefins (COCs) [60–68], biobased conjugated dienes [69,70], disubstituted α-olefins [44,71–74], and aromatic vinyl monomers [34,41,56,58,59], ethylene/α-olefin copolymers containing hydroxy group [44] etc. More recently, we realized that the catalysts containing unsymmetric iminoimidazolide ligands exhibited promising capabilities for synthesis of COCs [184]. Moreover, modification of phenoxide para-position enhanced the activity in ethylene polymerization and the copolymerization with α-olefin [45]. These results strongly suggest that the catalysts of this type will continue to contribute the development of new polyolefins. Moreover, this manuscript introduces analysis of catalytically active species through XAS (X-ray absorption spectroscopy). We highly hope that the analysis method can be used for more researchers in the near future for better understanding in catalysis cycle.

Author Contributions: Conceptualization, supervision, project administration, funding acquisition, data curation, KN; writing—original draft preparation, visualization, KN and KJ.; writing—review and editing, KN. All authors have read and agreed to the published version of the manuscript.

Funding: The projects by KN were partly supported by Grant-in-Aid for Scientific Research from the Japan Society for the Promotion of Science (JSPS, Nos. 13555253, 18350055, 21350054, 24350049, 15H03812, 15K14225, 18H01982, 18K18981, 19KK0139, 21H01942, 25K01583), Grant-in-Aid for Scientific Research on Innovative Areas (No. 26105003, "3D Active-Site Science") from The Ministry of Education, Culture, Sports, Science and Technology (MEXT), Japan. The synchrotron XAFS analysis were performed at the SPring-8 beam lines of BL01B1 with the approval of Japan Synchrotron Radiation Research Institute (JASRI, 2017A1512, 2018A1245, 2019A1233, 2020A0618, 2021A1435, 2021B1594, 2022A1276, 2022B1669, 2023A1765).

Data Availability Statement: We encourage all authors of articles published in MDPI journals to share their research data. In this section, please provide details regarding where data supporting reported results can be found, including links to publicly archived datasets analyzed or generated during the study. Where no new data were created, or where data is unavailable due to privacy or ethical restrictions, a statement is still required. Suggested Data Availability Statements are available in section "MDPI Research Data Policies" at https://www.mdpi.com/ethics.

 doi:10.20944/preprints202601.2232.v1

Acknowledgments: KN thanks to Dr. S. Kikkawa and Prof. S. Yamazoe (Tokyo Metropolitan University, TMU) for big support in XAS analysis, and Prof. N. Nakatani (TMU) for support in computational analysis. KJ expresses Tokyo Metropolitan government (Tokyo Global Partner Scholarship Program) for pre-doctoral fellowship.

Conflicts of Interest: The authors declare no conflicts of interest.

References

1. Plastics Europe. *Plastics the Fast Facts 2025.* https://plasticseurope.org/knowledge-hub/plastics-the-fast-facts-2025/ (accessed January 2026).
2. Selected recent reviews and book chapter, see refs 2–8: Baier, M. C.; Zuideveld, M. A.; Mecking S. Post-metallocenes in the industrial production of polyolefins. *Angew. Chem. Int. Ed.* **2014**, *53* (37), 9722–9744. doi.org/10.1002/anie.201400799
3. Stürzel, M.; Mihan, S.; Mülhaupt, R. From multisite polymerization catalysis to sustainable materials and all-polyolefin composites. *Chem. Rev.* **2016**, *116* (3), 1398–1433. doi.org/10.1021/acs.chemrev.5b00310
4. van Doremaele, G.; van Duin, M.; Valla, M.; Berthoud, A. On the development of titanium κ^1-amidinate complexes, commercialized as keltan ACE™ technology, enabling the production of an unprecedented large variety of EPDM polymer structures. *J. Polym. Sci., Part A: Polym. Chem.* **2017**, *55* (18), 2877–2891. doi.org/10.1002/pola.28634
5. *Handbook of Transition Metal Polymerization Catalysts, 2nd Ed.*; Hoff, R., Ed.; John Wiley & Sons, Inc.: Hoboken, NJ, USA, 2018. doi.org/10.1002/9781119242277
6. Nomura, K.; Kitphaitun, S. In *Catalysis for a Sustainable Environment: Reactions, Processes and Applied Technologies*; Pombeiro, A. J. L., Sutradhar, M., Alegria, E. C. B. A., Eds.; John Wiley & Sons, Ltd.: Chichester, West Sussex, UK, 2024; pp 323–338. doi.org/10.1002/9781119870647.ch15
7. Tan, C.; Zhou, C.; Chen. C. Material properties of functional polyethylenes from transition-metal-catalyzed ethylene–polar monomer copolymerization. *Macromolecules* **2022**, *55* (6), 1910–1922. doi.org/10.1021/acs.macromol.2c00058
8. Chen, C. Designing catalysts for olefin polymerization and copolymerization: Beyond electronic and steric tuning. *Nat. Rev. Chem.* **2018**, *2*, 6–14. doi.org/10.1038/s41570-018-0003-0
9. Selected pioneering reviews for metallocene catalysts, see refs 9–12: Brintzinger, H. H.; Fischer, D.; Mülhaupt, R.; Rieger, B.; Waymouth R. M. Stereospecific olefin polymerization with chiral metallocene catalysts. *Angew. Chem., Int. Ed. Engl.*, **1995**, *34* (11), 1143–1170. doi.org/10.1002/anie.199511431
10. Kaminsky, W. New polymers by metallocene catalysis. *Macromol. Chem. Phys.* **1996**, *197* (12), 3907–3945. doi.org/10.1002/macp.1996.021971201
11. Kaminsky, W.; Arndt, M. Metallocenes for polymer catalysis. *Adv. Polym. Sci.* **1997**, *127*, 143–187. doi.org/10.1007/BFb0103631
12. Suhm, J.; Heinemann, J.; Wörner, C.; Müller, P.; Stricker, F.; Kressler, J.; Okuda, J.; Mülhaupt, R. Novel polyolefin materials via catalysis and reactive processing. *Macromol. Symp.* **1998**, *129* (1), 1–28. doi.org/10.1002/masy.19981290103
13. Pioneering reviews for linked half-titanocene catalysts, see refs 12,13: McKnight, A. L.; Waymouth, R. M. Group 4 *ansa*-cyclopentadienyl-amido catalysts for olefin polymerization. *Chem. Rev*. **1998**, *98* (7), 2587–2598. doi.org/10.1021/cr940442r
14. Selected reviews for modified half-titanocene catalysts, refs. 4,6,14–17: Nomura, K.; Liu, J.; Padmanabhan, S.; Kitiyanan, B. Nonbridged half-metallocenes containing anionic ancillary donor ligands: New promising candidates as catalysts for precise olefin polymerization. *J. Mol. Catal. A: Chem.* **2007**, *267* (1–2), 1–29. doi.org/10.1016/j.molcata.2006.11.006
15. Nomura, K. Half-titanocenes containing anionic ancillary donor ligands as promising new catalysts for precise olefin polymerization. *Dalton Trans.* **2009**, (41), 8811–8823. doi.org/10.1039/B910407K
16. Nomura, K.; Liu, J. Half-titanocenes for precise olefinpolymerisation: Effects of ligand substituents and some mechanistic aspects. *Dalton Trans.* **2011**, *40* (30), 7666–7682. doi.org/10.1039/C1DT10086F

 doi:10.20944/preprints202601.2232.v1

17. Nomura, K.; Liu, J. In *Organometallic Reactions and Polymerisation*; Osakada, K., Ed.; The Lecture Notes in Chemistry, vol. 85; Springer: Berlin, 2014; pp 51–88.
18. Selected reviews for called post metallocene catalysts, refs. 2,7,8,18–20: Britovsek, G. J. P.; Gibson, V. C.; Wass, D. F. The search for new-generation olefin polymerization catalysts: Life beyond metallocenes. *Angew. Chem., Int. Ed. Engl.* **1999**, *38* (4), 428–447. doi.org/10.1002/(SICI)1521-3773(19990215)38:4<428::AID-ANIE428>3.0.CO;2-3
19. Gibson, V. C.; Spitzmesser, S. K. Advances in non-metallocene olefin polymerization catalysis. *Chem. Rev.* **2003**, *103* (1), 283–316. doi.org/10.1021/cr980461r
20. Coates, G. W.; Hustad, P. D.; Reinartz, S. Catalysts for the living insertion polymerization of alkenes: Access to new polyolefin architectures using Ziegler-Natta chemistry. *Angew. Chem. Int. Ed.* **2002**, *41*, 2236–2257. doi.org/10.1002/1521-3773(20020703)41:13<2236::AID-ANIE2236>3.0.CO;2-3
21. Delferro M.; Marks T. J. Multinuclear olefin polymerization catalysts. *Chem. Rev.*, **2011**, *111* (3), 2450–2485. doi.org/10.1021/cr1003634
22. McInnis, J. P.; Delferro, M.; Marks, T. J. Multinuclear group 4 catalysis: Olefin polymerization pathways modified by strong metal–metal cooperative effects. *Acc. Chem. Res.* **2014**, *47* (8), 2545–2557. doi.org/10.1021/ar5001633
23. Valente, A.; Mortreux, A.; Visseaux, M.; Zinck, P. Coordinative chain transfer polymerization. *Chem. Rev.* **2013**, *113* (5), 3836–3857. doi.org/10.1021/cr300289z
24. Macchioni, A. Ion pairing in transition-metal organometallic chemistry. *Chem. Rev.* **2005**, *105* (6), 2039–2074. doi.org/10.1021/cr0300439
25. Bochmann, M. The chemistry of catalyst activation: The case of group 4 polymerization catalysts. *Organometallics* **2010**, *29* (21), 4711–4740. doi.org/10.1021/om1004447
26. Kaminsky, W. Discovery of methylaluminoxane as cocatalyst for olefin polymerization. *Macromolecules* **2012**, *45* (8), 3289–3297. doi.org/10.1021/ma202453u
27. Yi, J.; Nakatani, N.; Nomura, K. Solution XANES and EXAFS analysis of active species of titanium, vanadium complex catalysts in ethylene polymerisation/dimerisation and syndiospecific styrene polymerization. *Dalton Trans*. **2020**, 49 (24), 8008–8028. doi.org/10.1039/D0DT01139H
28. Suhm, J.; Schneider M. J.; Mülhaupt, R. Influence of metallocene structures on ethene copolymerization with 1-butene and 1-octene. *J. Mol. Catal. A: Chem.*, **1998**, *128* (1–3), 215–227. doi.org/10.1016/S1381-1169(97)00175-1
29. Suhm, J.; Schneider, M. J.; Mülhaupt, R. Temperature dependence of copolymerization parameters in ethene/1-octene copolymerization using homogeneous *rac*-$Me_2Si(2\text{-}MeBenz[e]Ind)_2ZrCl_2$/MAO catalyst. *J. Polym. Sci. A* **1997**, *35* (4), 735–740. doi.org/10.1002/(SICI)1099-0518(199703)35:4<735::AID-POLA18>3.0.CO;2-O
30. For example, see refs 30-33: Canich, J. A. M.; Hlatky, G. G.; Turner, H. W. U.S. Patent 5,422,236, 1990.
31. Canich, J. A. M. U.S. Patent 5,026,798, 1991.
32. Stevens, J. C.; Timmers, F. J.; Wilson, D. R.; Schmidt, G. F.; Nickias, P. N.; Rosen, R. K.; Knight, G. W.; Lai, S.-Y. Eur. Pat. Appl. 416,815, 1991.
33. Stevens, J. C.; Neithamer, D. R. Eur. Pat. Appl. 418,022, 1991.
34. Nomura, K. In *Syndiotactic Polystyrene: Synthesis, Characterization, Processing, and Applications*; Schellenberg, J., Ed.; John Wiley & Sons, Inc.: Hoboken, NJ, 2010; pp 60–91.
35. Arriola, D. J.; Bokota, M.; Campbell Jr., R. E.; Klosin, J.; LaPointe, R. E.; Redwine, O. D.; Shankar, R. B.; Timmers, F. J.; Abboud, K. A. Penultimate effect in ethylene−styrene copolymerization and the discovery of highly active ethylene−styrene catalysts with increased styrene reactivity. *J. Am. Chem. Soc.* **2007**, *129* (22), 7065–7076. doi.org/10.1021/ja070061y
36. Guo, N.; Li, L.; Marks, T. J. Bimetallic catalysis for styrene homopolymerization and ethylene−styrene copolymerization: Exceptional comonomer selectivity and insertion regiochemistry. *J. Am. Chem. Soc.* **2004**, *126* (21), 6542–6543. doi.org/10.1021/ja048761f
37. Guo, N.; Stern, C. L.; Marks, T. J. Bimetallic effects in homopolymerization of styrene and copolymerization of ethylene and styrenic comonomers: Scope, kinetics, and mechanism. *J. Am. Chem. Soc.* **2008**, *130* (7), 2246–2261. doi.org/10.1021/ja076407m

 doi:10.20944/preprints202601.2232.v1

38. Tomotsu, N.; Ishihara, N.; Novel catalysts for syndiospecific polymerization of styrene. *Catal. Surv. Jpn.* **1997**, *1*, 89–110. doi.org/10.1023/A:1019072829203
39. Tomotsu, N.; Ishihara, N.; Newman, T. H.; Malanga, M. T. Syndiospecific polymerization of styrene. *J. Mol. Catal. A* **1998**, *128* (1–3), 167–190. doi.org/10.1016/S1381-1169(97)00171-4
40. Schellenberg, J. Recent transition metal catalysts for syndiotactic polystyrene. *Prog. Polym. Sci.* **2009**, *34* (8), 688–718. doi.org/10.1016/j.progpolymsci.2009.04.002
41. Zhang, H.; Nomura, K. Living copolymerization of ethylene with styrene catalyzed by (cyclopentadienyl)(ketimide)titanium(IV) complex−MAO catalyst system: Effect of anionic ancillary donor ligand. *Macromolecules* **2006**, *39* (16), 5266–5274. doi.org/10.1021/ma060503a
42. Nomura, K.; Naga, N.; Miki, M.; Yanagi, K.; Imai, A. Synthesis of various non-bridged Cp-aryloxy titanium(IV) complexes of the type CpTi(OAr)X_2, and the catalytic alkene polymerization: Important role of substituents on both aryloxy and cyclopentadienyl groups. *Organometallics* **1998**, *17* (11), 2152–2154. doi.org/10.1021/om980106r
43. Nomura, K.; Naga, N.; Miki, M.; Yanagi, K. Olefin polymerization by (cyclopentadienyl)(aryloxy)titanium(IV) complexes–cocatalyst system. *Macromolecules* **1998**, *31* (22), 7588–7597. doi.org/10.1021/ma980690f
44. Kitphaitun, S.; Yan, Q.; Nomura, K. Effect of $SiMe_3$, $SiEt_3$ *para*-substituents for exhibiting high activity, introduction of hydroxy group in ethylene copolymerization catalyzed by phenoxide-modified half-titanocenes. *Angew. Chem. Int. Ed*. **2020**, *59* (51), 23072–23076. doi.org/10.1002/anie.202010559
45. Gao, J.; Sun, W.-H.; Nomura, K. Synthesis of new phenoxide modified half-titanocene catalysts for ethylene polymerization. *Catalysts* **2025**, *15* (9), 840–851. doi.org/10.3390/catal15090840
46. Zhang, S.; Piers, W. E.; Gao, X.; Parvez, M. The mechanism of methane elimination in $B(C_6F_5)_3$-initiated monocyclopentadienyl-ketimide titanium and related olefin polymerization catalysts. *J. Am. Chem. Soc.* **2000**, *122* (23), 5499–5509. doi.org/10.1021/ja994378c
47. McMeeking, J.; Gao, X.; Spence, R. E. v. H.; Brown, S. J.; Jerermic, D. U.S. Patent 6,114,481, Sept 5, 2000.
48. Nomura, K.; Fujita, K.; Fujiki, M. Effects of cyclopentadienyl fragment in ethylene, 1-hexene, and styrene polymerizations catalyzed by half-titanocenes containing ketimide ligand of the type, Cp′TiCl2(NC^tBu_2). *Catal. Commun.* **2004**, *5* (8), 413–417. doi.org/10.1016/j.catcom.2004.05.005
49. Nomura, K.; Fujita, K.; Fujiki, M. Olefin polymerization by (cyclopentadienyl)(ketimide)titanium(IV) complexes of the type, Cp′$TiCl_2$(NC^tBu_2)-methylaluminoxane (MAO) catalyst systems. *J. Mol. Catal. A* **2004**, *220* (2), 133–144. doi.org/10.1016/j.molcata.2004.06.010
50. Dias, A. R.; Duarte, M. T.; Fernandes, A. C.; Fernandes, S.; Marques, M. M.; Martins, A. M.; da Silva, J. F.; Rodrigues, S. S. Titanium ketimide complexes as α-olefin homo- and copolymerisation catalysts: X-ray diffraction structures of [TiCp′(NC^tBu_2)Cl_2] (Cp′=Ind, Cp*). *J. Organomet. Chem.*, **2004**, *689* (1), 203–213. doi.org/10.1016/j.jorganchem.2003.10.005
51. Martins, A. M.; Marques, M. M.; Ascenso, J. R.; Dias, A. R.; Duarte, M. T.; Fernandes, A. C.; Fernandes, S.; Ferreira, M. J.; Matos, I.; Oliveira, M. C.; Rodrigues, S. S.; Wilson, C. *J.* Titanium and zirconium ketimide complexes: synthesis and ethylene polymerisation catalysis. *Organomet. Chem.* **2005**, *690* (4), 874–884. doi.org/10.1016/j.jorganchem.2004.10.030
52. Ferreira, M. J.; Martins, A. M. Group 4 ketimide complexes: Synthesis, reactivity and catalytic applications. *Coord. Chem. Rev.* **2006**, *250* (1–2), 118–132. doi.org/10.1016/j.ccr.2005.09.018
53. Ijpeij, E. G.; Zuideveld, M. A.; Arts, H. J.; van der Burgt, F.; van Doremaele, G. H. J. WO Patent 2007,031,295, 2007.
54. Ijpeij, E. G.; Windmuller, P. J. H.; Arts, H. J.; van der Burgt, F.; van Doremaele, G. H. J.; Zuideveld, M. A. WO Patent 2005,090,418, 2005.
55. Ijpeij, E. G.; Coussens, B.; Zuideveld, M. A.; van Doremaele, G. H. J.; Mountford, P.; Lutzc, M.; Spek, A. L. Synthesis, solid state and DFT structure and olefin polymerization capability of a unique base-free dimeric methyl titanium dication. *Chem. Commun*. **2010**, *46* (19), 3339–3341. doi.org/10.1039/B925781K
56. Nomura, K.; Komatsu, T.; Imanishi, Y. Syndiospecific styrene polymerization and efficient ethylene/styrene copolymerization catalyzed by (cyclopentadienyl)(aryloxy)titanium(IV) complexes−MAO system. *Macromolecules*, **2000**, *33* (22), 8122–8124. doi.org/10.1021/ma0011284

 doi:10.20944/preprints202601.2232.v1

57. Byun, D. J.; Fudo, A.; Tanaka, A.; Fujiki, M.; Nomura, K. Effect of cyclopentadienyl and anionic ancillary ligand in syndiospecific styrene polymerization catalyzed by nonbridged half-titanocenes containing aryloxo, amide, and anilide ligands: Cocatalyst systems. *Macromolecules* **2004**, *37* (15), 5520−5530. doi.org/10.1021/ma049549z
58. Nomura, K.; Okumura, H.; Komatsu, T.; Naga, N. Ethylene/styrene copolymerization by various (cyclopentadienyl)(aryloxy)titanium(IV) complexes−MAO catalyst systems. *Macromolecules* **2002**, *35* (14), 5388−5395. doi.org/10.1021/ma0200773
59. Aoki, H.; Nomura, K. Synthesis of amorphous ethylene copolymers with 2-vinylnaphthalene, 4-vinylbiphenyl and 1-(4-vinylphenyl)naphthalene. *Macromolecules* **2021**, *54* (1), 83−93. doi.org/10.1021/acs.macromol.0c02224
60. Nomura, K.; Tsubota, M.; Fujiki, M. Efficient ethylene/norbornene copolymerization by (Aryloxo)(indenyl)titanium(IV) complexes−MAO catalyst system. *Macromolecules* **2003**, *36* (11), 3797–3799. doi.org/10.1021/ma034215f
61. Nomura, K.; Wang, W.; Fujiki, M.; Liu, J. Notable norbornene (NBE) incorporation in ethylene–NBE copolymerization catalysed by nonbridged half-titanocenes: Better correlation between NBE incorporation and coordination energy. *Chem. Commun.* **2006**, (25), 2659–2661. doi.org/10.1039/B605005K
62. Apisuk, W.; Trambitas, A. G.; Kitiyanan, B.; Tamm, M.; Nomura, K. Efficient ethylene/norbornene copolymerization by half-titanocenes containing imidazolin-2-iminato ligands and MAO catalyst systems. *J. Polym. Sci., Part A: Polym. Chem.* **2013**, *51* (12), 2575–2580. doi.org/10.1002/pola.26638
63. Kawatsu, M.; Fujioka, T.; Losio, S.; Tritto, I.; Nomura, K. (Trialkylsilyl-cyclopentadienyl)titanium(IV) dichloride complexes containing ketimide ligands, Cp′$TiCl_2(N=C^tBu_2)$ (Cp′ = $Me_3SiC_5H_4$, $Et_3SiC_5H_4$), as efficient catalysts for ethylene copolymerisation with norbornene and tetracyclododecene. *Catal. Sci. Technol.* **2024**, *15* (9), 2757–2765. doi.org/10.1039/D5CY00160A
64. Apisuk, W.; Ito, H.; Nomura, K. Efficient synthesis of cyclic olefin copolymers with high glass transition temperatures by ethylene copolymerization with tetracyclododecene using (*tert*-BuC_5H_4)$TiCl_2(N=C^tBu_2)$–MAO Catalyst. *J. Polym. Sci., Part A: Polym. Chem.* **2016**, *54* (17), 2662–2667. doi.org/10.1002/pola.28144
65. Zhao, W.; Nomura, K. Copolymerizations of norbornene and tetracyclododecene with α-olefins by half-titanocene catalysts: Efficient synthesis of highly transparent, thermal resistance polymers. *Macromolecules* **2016**, *49* (1), 59–70. doi.org/10.1021/acs.macromol.5b02176
66. Okabe, M.; Nomura, K. Propylene/cyclic olefin copolymers with cyclopentene, cyclohexene, cyclooctene, tricyclo[6.2.1.0(2,7)]undeca-4-ene, and tetracyclododecene: The synthesis and effect of cyclic structure on thermal properties. *Macromolecules* **2023**, *56* (1), 81–91. doi.org/10.1021/acs.macromol.2c01966
67. Harakawa, H.; Okabe, M.; Nomura, K. The synthesis of cyclic olefin copolymers (COCs) by ethylene copolymerisations with cyclooctene, cycloheptene, and with tricyclo[6.2.1.0(2,7)]undeca-4-ene: The effect of cyclic monomer structures on thermal properties. *Polym. Chem.* **2020**, *11* (35), 5590–5600. doi.org/10.1039/D0PY00940G
68. Wang, W.; Fujiki, M.; Nomura, K. Copolymerization of ethylene with cyclohexene (CHE) catalyzed by nonbridged half-titanocenes containing aryloxo ligand: Notable effect of both cyclopentadienyl and anionic donor ligand for efficient CHE incorporation. *J. Am. Chem. Soc*. **2005**, *127* (13), 4582–4583. doi.org/10.1021/ja050274s
69. Kitphaitun, S.; Chaimongkolkunasin, S.; Manit, J.; Makino, R.; Kadota, J.; Hirano, H.; Nomura, K. Ethylene/myrcene copolymers as new bio-based elastomers prepared by coordination polymerization using titanium catalysts. *Macromolecules*, **2021**, *54* (21), 10049–10058. doi.org/10.1021/acs.macromol.1c01878
70. Guo, L.; Makino, R.; Shimoyama, D.; Kadota, J.; Hirano, H.; Nomura, K. Synthesis of ethylene/isoprene copolymers containing cyclopentane/cyclohexane units as unique elastomers by half-titanocene catalysts. *Macromolecules* **2023**, 56 (3), 899–914. doi.org/10.1021/acs.macromol.2c02399
71. Nomura, K.; Itagaki, K.; Fujiki, M. Efficient incorporation of 2-methyl-1-pentene in copolymerization of ethylene with 2-methyl-1-pentene catalyzed by nonbridged half-titanocenes. *Macromolecules* **2005**, *38* (6), 2053–2055. doi.org/10.1021/ma050277p

 doi:10.20944/preprints202601.2232.v1

72. Nomura, K.; Itagaki, K.; Efficient incorporation of vinylcylohexane in ethylene/vinylcyclohexane copolymerization catalyzed by nonbridged half-titanocenes. *Macromolecules* **2005**, *38* (20), 8121–8123. doi.org/10.1021/ma051439k
73. Itagaki, K.; Fujiki, M.; Nomura, K. Effect of cyclopentadienyl and anionic donor ligands on monomer reactivities in copolymerization of ethylene with 2-methyl-1-pentene by nonbridged half-titanocenes−cocatalyst systems. *Macromolecules* **2007**, *40* (18), 6489–6499. doi.org/10.1021/ma0700429
74. Khan, F. Z.; Kakinuki, K.; Nomura, K. Copolymerization of ethylene with *tert*-butylethylene using nonbridged half-titanocene-cocatalyst systems. *Macromolecules* **2009**, *42* (11), 3767–3773. doi.org/10.1021/ma900510d
75. Kitphaitun, S.; Fujimoto, T.; Ochi, Y.; Nomura, K. Effect of borate cocatalysts toward activity and comonomer incorporation in ethylene copolymerization by half-titanocene catalysts in methylcyclohexane. *ACS Org. Inorg. Au.* **2022**, *2* (5), 386–391. doi.org/10.1021/acsorginorgau.2c00020
76. Nomura, K.; Izawa, I.; Yi, J.; Nakatani, N.; Aoki, H.; Ina, T.; Mitsudome, T.; Tomotsu, N.; Yamazoe, S. Solution XAS analysis for exploring active species in syndiospecific styrene polymerization and 1-hexene polymerization using half-titanocene–MAO catalysts: Significant changes in the oxidation state in the presence of styrene. *Organometallics* **2019**, *38* (22), 4497–4507. doi.org/10.1021/acs.organomet.9b00638
77. Sun, Z.; Unruean, P.; Aoki, H.; Kitiyanan, B.; Nomura, K. Phenoxide-modified half-titanocenes supported on star-shaped ROMP polymers as efficient catalyst precursors for ethylene copolymerization. *Organometallics* **2020**, *39* (16), 2998–3009. doi.org/10.1021/acs.organomet.0c00365
78. Cherdron, H.; Brekner, M. -J.; Osan, F. Cycloolefin-copolymere: Eine neue klasse transparenter thermoplaste. *Angew. Makromol. Chem.* **1994**, *223* (1), 121–133. doi.org/10.1002/apmc.1994.052230109
79. Tritto, I.; Boggioni, L.; Ferro, D. R. Metallocene catalyzed ethene- and propene-*co*-norbornene polymerization: Mechanisms from a detailed microstructural analysis. *Coord. Chem. Rev.* **2006**, *250* (1–2), 212–241. doi.org/10.1016/j.ccr.2005.06.019
80. Nomura, K. Nonbridged half-titanocenes containing anionic ancillary donor ligands: Promising new catalysts for precise synthesis of cyclic olefin copolymers (COCs). *Chin. J. Polym. Sci.* **2008**, *26* (5), 513–523. doi.org/10.1142/S0256767908003217
81. Li, X.; Hou, Z. Organometallic catalysts for copolymerization of cyclic olefins. *Coord. Chem. Rev.* **2008**, *252* (15–17), 1842–1869. doi.org/10.1016/j.ccr.2007.11.027
82. Zhao, W.; Nomura, K. Design of efficient molecular catalysts for synthesis of cyclic olefin copolymers (COC) by copolymerization of ethylene and α-olefins with norbornene or tetracyclododecene. *Catalysts* **2016**, *6* (11), 175–190. doi.org/10.3390/catal6110175
83. Boggioni, L.; Tritto, I. State of the art of cyclic olefin polymers. *MRS Bull.* **2013**, *38*, 245–251. doi.org/10.1557/mrs.2013.53
84. Nomura, K. Development of half-titanocene catalysts for synthesis of cyclic olefin copolymers. *Polyolefin J.* **2023**, *10* (2), 59–70. doi.org/10.22063/poj.2023.3308.1250
85. Wang, W.; Qu, S.; Li, X.; Chen, J.; Guo, Z.; Sun, W.-H. Transition metal complex catalysts promoting copolymers of cycloolefin with propylene/higher olefins. *Coord. Chem. Rev.* **2023**, *494*, 215351. doi.org/10.1016/j.ccr.2023.215351
86. Zhao, Y.; Zhang, J.; Zhang, Y.; Cui, L.; Chi, Y.; Jian, Z. Advances in high refractive index cycloolefin-containing polymeric materials. *Macromolecules* **2025**, *58* (20), 10949–10962. doi.org/10.1021/acs.macromol.5c01915
87. Polyplastics. Topas: High-Performance Cyclic Olefin Copolymer. https://www.polyplastics.com/en/product/topas.vm (accessed January 2026).
88. Mitsui Chemicals. Apel™ Cyclic Olefin Copolymer. https://jp.mitsuichemicals.com/en/special/apel/ (accessed January 2026).
89. Selected initial reports, refs. 89-95: Ruchatz, D.; Fink, G. Ethene-norbornene copolymerization using homogeneous metallocene and half-sandwich catalysts: Kinetics and relationships between catalyst structure and polymer structure: 1. Kinetics of the ethene-norbornene copolymerization using the [(isopropylidene)(η^5-inden-1-ylidene-η^5-cyclopentadienyl)]zirconium dichloride/methylaluminoxane catalyst. *Macromolecules* **1998**, *31* (15), 4669–4673. doi.org/10.1021/ma971041r

 doi:10.20944/preprints202601.2232.v1

90. Ruchatz, D.; Fink, G. Ethene–norbornene copolymerization using homogenous metallocene and half-sandwich catalysts: Kinetics and relationships between catalyst structure and polymer structure: 2. Comparative study of different metallocene- and half-sandwich/methylaluminoxane catalysts and analysis of the copolymers by ^{13}C nuclear magnetic resonance spectroscopy. *Macromolecules* **1998**, *31* (15), 4674–4680. doi.org/10.1021/ma971042j
91. Arndt, M.; Beulich, I. C_1-Symmetric metallocenes for olefin polymerisation, 1. Catalytic performance of [Me_2C(3-^{tert}BuCp)(Flu)]$ZrCl_2$ in ethene/norbornene copolymerisation. *Macromol. Chem. Phys.* **1998**, *199* (6), 1221–1232. doi.org/10.1002/(SICI)1521-3935(19980601)199:6<1221::AID-MACP1221>3.0.CO;2-2
92. Provasoli, A.; Ferro, D. R.; Tritto, I.; Boggioni, L. The conformational characteristics of ethylene-norbornene copolymers and their influence on the ^{13}C NMR spectra. *Macromolecules* **1999**, *32* (20), 6697–6706. doi.org/10.1021/ma990739x
93. Tritto, I.; Marestin, C.; Boggioni, L.; Zetta, L.; Provasoli, A.; Ferro, D. R. Ethylene-norbornene copolymer microstructure: Assessment and advances based on assignments of ^{13}C NMR spectra. *Macromolecules* **2000**, *33* (24), 8931–8944. doi.org/10.1021/ma000795u
94. Tritto, I.; Marestin, C.; Boggioni, L.; Brintzinger, H. H.; Ferro, D. R. Stereoregular and stereoirregular alternating ethylene-norbornene copolymers. *Macromolecules* **2001**, *34* (11), 5770–5777. doi.org/10.1021/ma010122r
95. Tritto, I.; Boggioni, L.; Ferro, D. R. Alternating isotactic ethylene–norbornene copolymers by C_1-symmetric metallocenes: Determination of the copolymerization parameters and mechanistic considerations on the basis of pentad analysis. *Macromolecules* **2004**, *37* (26), 9681–9693. doi.org/10.1021/ma048502a
96. Selected initial reports, refs. 96-99: Harrington, B. A.; Crowther, D. J. Stereoregular, alternating ethylene–norbornene copolymers from monocyclopentadienyl catalysts activated with non-coordinating discrete anions. *J. Mol. Catal. A: Chem.* **1998**, *128* (1–3), 79–84. doi.org/10.1016/S1381-1169(97)00164-7
97. McKnight, A. L.; Waymouth, R. M. Ethylene/norbornene copolymerizations with titanium CpA catalysts. *Macromolecules* **1999**, *32* (9), 2816–2825. doi.org/10.1021/ma981365v
98. Thorshaug, K.; Mendichi, R.; Tritto, I.; Trinkle, S.; Friedrich, C.; Mülhaupt, R. Poly(ethene-*co*-norbornene) obtained with a constrained geometry catalyst. A study of reaction kinetics and copolymer properties. *Macromolecules* **2002**, *35* (8), 2903–2911. doi.org/10.1021/ma011949o
99. Hasan, T.; Ikeda, T.; Shiono, T. Ethene–norbornene copolymer with high norbornene content produced by *ansa*-fluorenylamidodimethyltitanium complex using a suitable activator. *Macromolecules* **2004**, *37* (23), 8503–8509. doi.org/10.1021/ma048492d
100. Selected initial reports, refs. 100-105: Altamura, P.; Grassi, A. Crystalline alternating sequences identified in ethylene-*co*-norbornene polymers produced by the (η^5-$C_2B_9H_{11}$)$Zr(NEt_2)_2$($NHEt_2$)-Al^iBu_3 catalyst. *Macromolecules* **2001**, *34* (26), 9197–9200. doi.org/10.1021/ma011138k
101. Yoshida, Y.; Mohri, J.; Ishii, S.; Mitani, M.; Saito, J.; Matsui, S.; Makio, H.; Nakano, T.; Tanaka, H.; Onda, M.; Yamamoto, Y.; Mizuno, A.; Fujita, T. Living copolymerization of ethylene with norbornene catalyzed by bis(pyrrolide–imine) titanium complexes with MAO. *J. Am. Chem. Soc.* **2004**, *126* (38), 12023–12032. doi.org/10.1021/ja048357g
102. Li, X.-F.; Dai, K.; Ye, W.-P.; Pan, L.; Li, Y.-S. New titanium complexes with two β-enaminoketonato chelate ligands: Syntheses, structures, and olefin polymerization activities. *Organometallics* **2004**, *23* (6), 1223–1230. doi.org/10.1021/om030396y
103. Marconi, R.; Ravasio, A.; Boggioni, L.; Tritto, I. Silyl-terminated ethylene-*co*-norbornene copolymers by organotitanium-based catalysts. *Macromol. Rapid Commun.* **2009**, *30* (1), 39–44. doi.org/10.1002/marc.200800559
104. He, L. P.; Liu, J. L.; Li, Y. G.; Liu, S. R.; Li, Y. S. High-temperature living copolymerization of ethylene with norbornene by titanium complexes bearing bidentate [O, P] ligands. *Macromolecules* **2009**, *42* (21), 8566–8570. doi.org/10.1021/ma901285a
105. Yang, X. H.; Wang, Z.; Sun, X. L.; Tang, Y. Synthesis, characterization, and catalytic behaviours of β-carbonylenamine-derived [O^-NS]$TiCl_3$ complexes in ethylene homo- and copolymerization. *Dalton Trans.* **2009**, (41), 8945–8954. doi.org/10.1039/B910868H

 doi:10.20944/preprints202601.2232.v1

106. For example, Mitsui Chemicals Co. Production of Cyclic Olefin Copolymers with Tetracyclododecene (TCD) Using Vanadium Catalysts. Jpn. Pat. JP 2001-106730, 2001; Jpn. Pat. JP 2006-022266, 2006; Jpn. Pat. JP 2008-248171, 2008.
107. Kaminsky, W.; Bark, A. Copolymerization of ethene and dimethanooctahydronaphthalene with aluminoxane containing catalysts. *Polym. Int*. **1992**, *28* (3), 251–253. doi.org/10.1002/pi.4990280312
108. Kaminsky, W.; Engehausen, R.; Kopf, J. A tailor-made metallocene for the copolymerization of ethene with bulky cycloalkenes. *Angew. Chem. Int. Ed. Engl*. **1995**, *34* (20), 2273–2275. doi.org/10.1002/anie.199522731
109. Goodall, B. L.; McIntosh, L. H.; Rhodes, L. F. New catalysts for the polymerization of cyclic olefins. *Macromol. Symp*. **1995**, *89* (1), 421–432. doi.org/10.1002/masy.19950890139
110. Donner, M.; Fernandes, M.; Kaminsky, W. Synthesis of copolymers with sterically hindered and polar monomers. *Macromol. Symp*. **2006**, *236* (1), 193–202. doi.org/10.1002/masy.200690055
111. Selected initial reports, see refs 111-114: Hasan, T.; Ikeda, T.; Shiono, T. Random Copolymerization of propene and norbornene with *ansa*-fluorenylamidodimethyltitanium-based catalysts. *Macromolecules* **2005**, *38* (4), 1071–1074. doi.org/10.1021/ma0481171
112. Cai, Z.; Nakayama, Y.; Shiono, T. Living random copolymerization of propylene and norbornene with *ansa*-fluorenylamidodimethyltitanium complex: Synthesis of novel syndiotactic polypropylene-*b*-poly(propylene-*ran*-norbornene). *Macromolecules* **2006**, *39* (6), 2031–2033. doi.org/10.1021/ma060122x
113. Shiono, T.; Sugimoto, M.; Hasan, T.; Cai, Z.; Ikeda, T. Random copolymerization of norbornene with higher 1-alkene with *ansa*-fluorenylamidodimethyltitanium catalyst. *Macromolecules* **2008**, *41* (22), 8292–8294. doi.org/10.1021/ma802119d
114. Cai, Z.; Harada, R.; Nakayama, Y.; Shiono, T. Highly active living random copolymerization of norbornene and 1-alkene with *ansa*-fluorenylamidodimethyltitanium derivative: Substituent effects on fluorenyl ligand. *Macromolecules* **2010**, *43* (10), 4527–4531. doi.org/10.1021/ma1006107
115. Pino, P.; Giannini, U.; Porri, L. In *Encyclopedia of Polymer Science and Engineering*, 2nd ed.; Mark, H. F., Bikales, N. M., Overberger, C. C., Menges, G., Eds.; Wiley-Interscience: New York, 1987; Vol. 8, pp 155–179.
116. Kaminsky, W.; Bark, A.; Spiehl, R.; Möller-Linderhof, N.; Niedoba, S. In *Transition Metals and Organometallics as Catalysts for Olefin Polymerization*; Kaminsky, W., Sinn, H., Eds.; Springer-Verlag: Berlin, 1988; pp 291–301.
117. Shaffer, T. D.; Canich, J. A. M.; Squire, K. R. metallocene-catalyzed copolymerization of ethylene and isobutylene to substantially alternating copolymers. *Macromolecules* **1998**, *31* (15), 5145–5147. doi.org/10.1021/ma980196b
118. Nakayama,Y.; Sogo, Y.; Cai, Z.; Shiono, T. Copolymerization of ethylene with 1,1-disubstituted olefins catalyzed by ansa-(fluorenyl)(cyclododecylamido)dimethyltitanium complexes. *J. Polym. Sci., Part A: Polym. Chem.* **2013**, *51* (5), 1223–1229. doi.org/10.1002/pola.26491
119. Li, H.; Li, L.; Marks, T. J.; Liable-Sands. L.; Rheingold, A. L. Catalyst/cocatalyst nuclearity effects in single-site olefin polymerization. significantly enhanced 1-octene and isobutene comonomer enchainment in ethylene polymerizations mediated by binuclear catalysts and cocatalysts. *J. Am. Chem. Soc.* **2003**, *125* (36), 10788–10789. doi.org/10.1021/ja036289c
120. Li, H.; Li, L.; Schwartz, D. J.; Metz, M. V.; Marks, T. J.; Liable-Sands. L.; Rheingold, A. L. Coordination copolymerization of severely encumbered isoalkenes with ethylene: enhanced enchainment mediated by binuclear catalysts and cocatalysts. *J. Am. Chem. Soc.* **2005**, *127* (42), 14756–14768. doi.org/10.1021/ja052995x
121. Nomura, K.; Kakinuki, K.; Fujiki, M.; Itagaki, K. Direct precise functional group introduction into polyolefins: Efficient incorporation of vinyltrialkylsilanes in ethylene copolymerizations by nonbridged half-titanocenes. *Macromolecules*, **2008**, *41* (23), 8974–8976. doi.org/10.1021/ma8020757
122. Gao, Y.; Chen, J.; Wang, Y.; Pickens, D. B.; Motta, A.; Wang, Q. J.; Chung, Y.-W.; Lohr, T. L.; Marks, T. J. Highly branched polyethylene oligomers via group IV-catalysed polymerization in very nonpolar media. *Nat. Catal.* **2019**, *2*, 236–242. doi.org/10.1038/s41929-018-0224-0
123. Sian, L.; Dall'Anese, A.; Macchioni, A.; Tensi, L.; Busico, V.; Cipullo, R.; Goryunov, G. P.; Uborsky, D.; Voskoboynikov, A. Z.; Ehm, C.; Rocchigiani, L.; Zuccaccia, C. Role of solvent coordination on the structure and dynamics of *ansa*-zirconocenium ion pairs in aromatic hydrocarbons. *Organometallics* **2022**, *41* (5), 547–560. doi.org/10.1021/acs.organomet.1c00653

 doi:10.20944/preprints202601.2232.v1

124. Baumann, R.; Davis, W. M.; Schrock, R. R. Synthesis of titanium and zirconium complexes that contain the tridentate diamido ligand, [((*t*-Bu-*d*$_6$)N-*o*-C$_6$H$_4$)$_2$O]$^{2-}$ ([NON]$^{2-}$) and the living polymerization of 1-hexene by activated [NON]ZrMe$_2$. *J. Am. Chem. Soc.* **1997**, *119* (16), 3830–3831. doi.org/10.1021/ja963823q
125. Gandini, A. Polymers from renewable resources: A challenge for the future of macromolecular materials. *Macromolecules* **2008**, *41* (24), 9491–9504. doi.org/10.1021/ma801735u
126. Coates, G. W.; Hillmyer, M. A. A virtual issue of Macromolecules: Polymers from renewable resources. *Macromolecules* **2009**, *42* (21), 7987–7989. doi.org/10.1021/ma902107w
127. Yao, K.; Tang, C. Controlled polymerization of next-generation renewable monomers and beyond. *Macromolecules* **2013**, *46* (5), 1689–1712. doi.org/10.1021/ma3019574
128. Satoh, K. Controlled/living polymerization of renewable vinyl monomers into bio-based polymers. *Polym. J.* **2015**, *47*, 527–536. doi.org/10.1038/pj.2015.31
129. Wang, Z.; Yuan, L.; Tang, C. Sustainable elastomers from renewable biomass. *Acc. Chem. Res.* **2017**, *50* (7), 1762–1773. doi.org/10.1021/acs.accounts.7b00209
130. *Polymers from Plant Oils*, 2nd ed.; Gandini, A., Lacerda, T. M., Eds.; John Wiley & Sons, Inc.: Hoboken, NJ; Scrivener Publishing LLC: Beverly, MA, 2019.
131. Fagnani, D. E.; Tami, J. L.; Copley, G.; Clemons, M. N.; Getzler, Y. D. Y. L.; McNeil, A. J.; 100th Anniversary of macromolecular science viewpoint: Redefining sustainable polymers. *ACS Macro Lett.* **2021**, *10* (1), 41–53. doi.org/10.1021/acsmacrolett.0c00789
132. Haque, F. M.; Ishibashi, J. S. A. A.; Lidston, C. A. L. L.; Shao, H.; Bates, F. S.; Chang, A. B.; Coates, G. W.; Cramer, C. J.; Dauenhauer, P. J.; Dichtel, W. R.; Ellison, C. J.; Gormong, E. A.; Hamachi, L. S.; Hoye, T. R.; Jin, M; Kalow, J. A. Kim, H. J.; Kumar, G.; LaSalle, C. J.; Liffland, S.; Lipinski, B. M.; Pang, Y.; Parveen, R.; Peng, X.; Popowski, V.; Prebihalo, E. A.; Reddi, Y.; Reineke, T. M.; Sheppard, D. T.; Swartz, J. L.; Tolman, W. B.; Vlaisavljevich, B.; Wissinger, J.; Xu, S.; Hillmyer, M. A. Defining the macromolecules of tomorrow through synergistic sustainable polymer research. *Chem. Rev.* **2022**, *122* (6), 6322–6373. doi.org/10.1021/acs.chemrev.1c00173
133. Wilbon, P. A.; Chu, F.; Tang, C. Progress in renewable polymers from natural terpenes, terpenoids, and rosin. *Macromol. Rapid Comm.* **2013**, *34* (1), 8–37. doi.org/10.1002/marc.201200513
134. Thomsett, M. R.; Storr, T. E.; Monaphan, O. R.; Stockman, R. A.; Howdle, S. M. Progress in the synthesis of sustainable polymers from terpenes and terpenoids. *Green Materials* **2016**, *4* (3), 115–134. doi.org/10.1680/jgrma.16.00009
135. Kawamura, K.; Nomura, K. Ethylene copolymerization with limonene and β-pinene: new bio-based polyolefins prepared by coordination polymerization. *Macromolecules* **2021**, *54* (10), 4693–4703. doi.org/10.1021/acs.macromol.1c00559
136. Ren, X.; Guo, F.; Fu, H.; Song, Y.; Li, Y.; Hou, Z. Scandium-catalyzed copolymerization of myrcene with ethylene and propylene: Convenient syntheses of versatile functionalized polyolefins. *Polym. Chem.* **2018**, *9* (10), 1223–1233. doi.org/10.1039/C8PY00039E
137. For example, refs. 137-143: Georges, S.; Touré, A. O.; Visseaux, M.; Zinck, P. Coordinative chain transfer copolymerization and terpolymerization of conjugated dienes. *Macromolecules* **2014**, *47* (14), 4538–4547. doi.org/10.1021/ma5008896
138. Liu, B.; Li, L.; Sun, G.; Liu, D.; Li, S.; Cui, D. Isoselective 3,4-(co)polymerization of bio-renewable myrcene using NSN-ligated rare-earth metal precursor: an approach to a new elastomer. *Chem. Commun.* **2015**, *51* (6), 1039–1041. doi.org/10.1039/C4CC08962F
139. Naddeo, M.; Buonerba, A.; Luciano, E.; Grassi, A.; Proto, A.; Capacchione, C. Stereoselective polymerization of biosourced terpenes β-myrcene and β-ocimene and their copolymerization with styrene promoted by titanium catalysts. *Polymer* **2017**, *131*, 151–159. doi.org/10.1016/j.polymer.2017.10.028
140. Laur, E.; Welle, A.; Vantomme, A.; Brusson, J.-M.; Carpentier, J.-F.; Kirillov, E. Stereoselective copolymerization of styrene with terpenes catalyzed by an *ansa*-lanthanidocene catalyst: Access to new syndiotactic polystyrene-based materials. *Catalysts* **2017**, *7* (12), 361–372. doi.org/10.3390/catal7120361
141. Li, W.; Zhao, J.; Zhang, X.; Gong, D. Capability of PN$_3$-type cobalt complexes toward selective (co-)polymerization of myrcene, butadiene, and isoprene: Access to biosourced polymers. *Ind. Eng. Chem. Res.* **2019**, *58* (8), 2792–2800. doi.org/10.1021/acs.iecr.8b05866

 doi:10.20944/preprints202601.2232.v1

142. González-Zapata, J. L.; Enríquez-Medrano, F. J.; López González, H. R.; Revilla-Vázquez, J.; Carrizales, R. M.; Georgouvelas, D.; Valencia, L.; Díaz de León Gómez, R. E. Introducing random bio-terpene segments to high *cis*-polybutadiene: making elastomeric materials more sustainable. *RSC Adv.* **2020**, *10* (72), 44096–44102. doi.org/10.1039/D0RA09280K
143. Lamparelli, D. H.; Paradiso, V.; Monica, F. D.; Proto, A.; Guerra, S.; Giannini, L.; Capacchione, C. Toward more sustainable elastomers: Stereoselective copolymerization of linear terpenes with butadiene. *Macromolecules* **2020**, *53* (5), 1665–1673. doi.org/10.1021/acs.macromol.9b02646
144. Talsi, E.; Bryliakov, K. *Application of EPR and NMR Spectroscopy in Homogeneous Catalysis*; CRC Press, Taylor & Francis: Boca Raton, FL, USA, 2017.
145. Goswami, M.; Chirila, A.; Rebreyend, C.; de Bruin, B. EPR spectroscopy as a tool in homogeneous catalysis research. *Top Catal.* **2015**, *58*, 719–750. doi.org/10.1007/s11244-015-0414-9
146. Boča, R. Zero-field splitting in metal complexes. *Coord. Chem. Rev.* **2004**, *248*, 757–815. doi.org/10.1016/j.ccr.2004.03.001
147. Krzystek, J.; Ozarowski, A.; Telser, J.; Crans, D. C. High-frequency and -field electron paramagnetic resonance of vanadium(IV, III, and II) complexes. *Coord. Chem. Rev.* **2015**, *301–302*, 123–133. doi.org/10.1016/j.ccr.2014.10.014
148. Selected initial reports, see refs 148-159: Nomura, K.; Mitsudome, T.; Yamazoe, S. Direct observation of catalytically active species in reaction solution by x-ray absorption spectroscopy (XAS). *Jpn. J. Appl. Phys.* **2019**, *58*, 100502. doi.org/10.7567/1347-4065/ab3e5c
149. Nomura, K. Solution x-ray absorption spectroscopy (XAS) for analysis of catalytically active species in reactions with ethylene by homogeneous (imido)vanadium(V) complexes–Al cocatalyst systems. *Catalysts* **2019**, *9* (12), 1016. doi.org/10.3390/catal9121016
150. Bartlett, S. A.; Moulin, J.; Tromp, M.; Reid, G.; Dent, A. J.; Cibin, G.; McGuinness, D. S.; Evans, J. Activation of [$CrCl_3${R-SN(H)S-R}] catalysts for selective trimerization of ethene: A freeze-quench Cr K-edge XAFS study. *ACS Catal.* **2014**, *4* (11), 4201–4204. doi.org/10.1021/cs501017g
151. Takaya, H.; Nakajima, S.; Nakagawa, N.; Isozaki, K.; Iwamoto, T.; Imayoshi, R.; Gower, N. J.; Adak, L.; Hatakeyama, T.; Honma, T.; Takagaki, M.; Sunada, Y.; Nagashima, H.; Hashizume, D.; Takahashi, O.; Nakamura, M. *Bull. Chem. Soc. Jpn.* **2015**, *88* (33), 410–418. doi.org/10.1246/bcsj.20140376
152. Nomura, K.; Mitsudome, T.; Igarashi, A.; Nagai, G.; Tsutsumi, K.; Ina, T.; Omiya, T.; Takaya, H.; Yamazoe, S. Synthesis of (adamantylimido)vanadium(V) dimethyl complex containing (2-anilidomethyl)pyridine ligand and selected reactions: Exploring the oxidation state of the catalytically active species in ethylene dimerization. *Organometallics* **2017**, *36* (3), 530–542. doi.org/10.1021/acs.organomet.6b00727
153. Nagai, G.; Mitsudome, T.; Tsutsumi, K.; Sueki, S.; Ina, T.; Tamm, M.; Nomura, K. Effect of Al cocatalyst in ethylene and ethylene/norbornene (co)polymerization by (imido)vanadium dichloride complexes containing anionic N-heterocyclic carbenes having weakly coordinating borate moiety. *J. Jpn. Petrol. Inst.* **2017**, *60* (5), 256–262. doi.org/10.1627/jpi.60.256
154. Nomura, K.; Oshima, M.; Mitsudome, T.; Harakawa, H.; Hao, P.; Tsutsumi, K.; Nagai, G.; Ina, T.; Takaya, H.; Sun, W. -H.; Yamazoe, S. Synthesis and structural analysis of (imido)vanadium dichloride complexes containing 2-(2′-benz-imidazolyl)pyridine ligands: effect of al cocatalyst for efficient ethylene (co)polymerization. *ACS Omega* **2017**, *2* (12), 8660−8673. doi.org/10.1021/acsomega.7b01225
155. Nomura, K.; Tsutsumi, K.; Nagai, G.; Omiya, T.; Ina, T.; Yamazoe, S.; Mitsudome, T. S. Solution XAS analysis of various (imido)vanadium(V) dichloride complexes containing monodentate anionic ancillary donor ligands: Effect of aluminium cocatalyst in ethylene/norbornene (co)polymerization. *J. Jpn. Petrol. Inst.* **2018**, *61* (5), 282−287. doi.org/10.1627/jpi.61.282
156. Kuboki, M.; Nomura, K. (Arylimido)niobium(V) complexes containing 2-pyridylmethylanilido ligand as catalyst precursors for ethylene dimerization that proceeds via cationic Nb(V) species. *Organometallics* **2019**, *38* (7), 1544−1559. doi.org/10.1021/acs.organomet.9b00017
157. Hirano, M.; Sano, K.; Kanazawa, Y.; Komine, N.; Maeno, Z.; Mitsudome T.; Takaya, H. Mechanistic insights on pd/cu-catalyzed dehydrogenative coupling of dimethyl phthalate. *ACS Catal.* **2018**, *8* (7), 5827−5841. doi.org/10.1021/acscatal.8b01095

 doi:10.20944/preprints202601.2232.v1

158. Nomura, K.; Nagai, G.; Izawa, I.; Mitsudome, T.; Tamm, M.; Yamazoe, S. XAS analysis of reactions of (arylimido)vanadium(v) dichloride complexes containing anionic NHC that contains a weakly coordinating $B(C_6F_5)_3$ moiety (WCA-NHC) or phenoxide ligands with Al alkyls: A Potential ethylene polymerization catalyst with WCA-NHC ligands. *ACS Omega* **2019**, *4* (20), 18833−18845. doi.org/10.1021/acsomega.9b02828
159. Agata, R.; Takaya, H.; Matsuda, H.; Nakatani, N.; Takeuchi, K.; Iwamoto, T.; Hatakeyama, T.; Nakamura, N. Iron-catalyzed cross coupling of aryl chlorides with alkyl grignard reagents: Synthetic scope and Fe^{II}/Fe^{IV} Mechanism supported by x-ray absorption spectroscopy and density functional theory calculations. *Bull. Chem. Soc. Jpn.* **2019**, *92* (2), 381−390. doi.org/10.1246/bcsj.20180333
160. For examples, refs. 160-164: Thomas, J. M.; Sankar, G. *J.* The role of XAFS in the in situ and ex situ elucidation of active sites in designed solid catalysts. *Synch. Rad.* **2001**, *8*, 55−60. doi.org/10.1107/S090904950001935X
161. Dent, A. J. Development of time-resolved XAFS instrumentation for quick EXAFS and energy-dispersive EXAFS measurements on catalyst systems. *Top. Catal.* **2002**, *18*, 27−35. doi.org/10.1023/A:1013826015970
162. Thomas, J. M.; Catlow, C. R. A.; Sankar, G. Determining the structure of active sites, transition states and intermediates in heterogeneously catalysed reactions. *Chem. Commun.* **2002**, *24*, 2921−2925. doi.org/10.1039/B210679P
163. Bare, S. R.; Ressler, T. Chapter 6 characterization of catalysts in reactive atmospheres by X-ray absorption spectroscopy. *Adv. Catal.* **2009**, *52*, 339−465. doi.org/10.1016/S0360-0564(08)00006-0
164. *XAFS Techniques for Catalysts, Nanomaterials, and Surfaces*; Iwasawa, Y., Asakura, K., Tada, M., Eds.; Springer: Cham, Switzerland, 2017.
165. Srivastava, U. C.; Nigam, H. L. X-ray absorption edge-structure of compounds of some transition elements. *Coord. Chem. Rev.* **1973**, *9* (3–4), 275–310.
166. Wong, J.; Lytle, F. W.; Messmer, R. P.; Maylotte, D. H. *K*-edge absorption spectra of selected vanadium compounds. *Phys. Rev. B*. **1984**, *30*, 5596−5610. doi.org/10.1103/PhysRevB.30.5596
167. Wu, Z.; Xian, D. C.; Natoli, C. R.; Marceli, A.; Paris, E.; Mottana, A. Symmetry dependence of x-ray absorption near-edge structure at the metal edge of transition metal compounds. *Appl. Phys. Lett.* **2001**, *79* (12), 1918−1920. doi.org/10.1063/1.1405149
168. Rehr, J. J.; Ankudinov, A. L. Progress in the theory and interpretation of XANES. *Coord. Chem. Rev.* **2005**, *249* (1−2), 131−140. doi.org/10.1016/j.ccr.2004.02.014
169. Yamamoto, T. Assignment of pre-edge peaks in K-edge x-ray absorption spectra of 3d transition metal compounds: electric dipole or quadrupole?. *X-Ray Spectrom.* **2008**, *37* (6), 572−584. doi.org/10.1002/xrs.1103
170. Glatzel, P.; Smolentsev, G.; Bunker, G. The electronic structure in 3d transition metal complexes: Can we measure oxidation states?. *J. Phys.: Conf. Ser.* **2009**, *190*, 012046. doi.org/10.1088/1742-6596/190/1/012046
171. Yi, J.; Nakatani, N.; Nomura, K.; Hada, M. Time-dependent DFT study of the K-edge spectra of vanadium and titanium complexes: effects of chloride ligands on pre-edge features. *Phys. Chem. Chem. Phys*. **2020**, *22* (2), 674−682. doi.org/10.1039/C9CP05891E
172. Yokoyama, T.; Kosugi, N.; Kuroda, H. Polarized xanes spectra of $CuCl_2 \cdot 2H_2O$: Further evidence for shake-down phenomena. *Chem. Phys*. **1986**, *103* (1), 101−109. doi.org/10.1016/0301-0104(86)85106-0
173. Bair, R. A.; Goddard III, W. A. Ab initio studies of the x-ray absorption edge in copper complexes: I. Atomic Cu^{2+} and Cu(II)Cl_2. *Phys. Rev. B* **1980**, *22*, 2767−2776. doi.org/10.1103/PhysRevB.22.2767
174. Hu, P.; Hu, P.; Vu, T. D.; Li, M.; Wang, S.; Ke, Y.; Zeng, X.; Mai, L.; Long, Y. Vanadium oxide: Phase diagrams, structures, synthesis, and applications. *Chem.Rev*. **2023**, *123* (8), 4353−4415. doi.org/10.1021/acs.chemrev.2c00546
175. Asakura, H.; Shishido, T.; Yamazoe, S.; Teramura, K.; Tanaka, T. Structural analysis of group V, VI, and VII metal compounds by XAFS. *J. Phys. Chem. C* **2011**, *115* (48), 23653−23663. doi.org/10.1021/jp2034104
176. Yamamoto, T. What is the origin of pre-edge peaks in K-edge XANES spectra of 3d transition metals: electric dipole or quadrupole?. *Adv. X-Ray. Chem. Anal. Japan* **2007**, *38*, 45−65.
177. Grassi, A.; Zambelli, A.; Laschi, F. Reductive decomposition of cationic half-titanocene(IV) complexes, precursors of the active species in syndiospecific styrene polymerization. *Organometallics* **1996**, *15* (2), 480−482. doi.org/10.1021/om950666f

 doi:10.20944/preprints202601.2232.v1

178. Minieri, G.; Corradini, P.; Guerra, G.; Zambelli, A.; Cavallo, L. A theoretical study of syndiospecific styrene polymerization with Cp-based and Cp-free titanium catalysts: 2. Mechanism of chain-end stereocontrol. *Macromolecules* **2001**, *34*, 5379−5385. doi.org/10.1021/ma002163d
179. Mahanthappa, M. K.; Waymouth, R. M. Titanium-mediated syndiospecific styrene polymerizations: Role of oxidation state. *J. Am. Chem. Soc.* **2001**, *123*, 12093−12094. doi.org/10.1021/ja016521j
180. Tomotsu, N.; Shozaki, H.; Aida, M.; Takeuchi, M.; Yokota, K.; Aoyama, Y.; Ikeuchi, S.; Inoue, T. In *Future Technology for Polyolefin and Olefin Polymerization Catalysis*; Terano, M., Shiono, T., Eds.; Technology and Education Publishers: Tokyo, 2002; pp 49–54
181. Zhang, H.; Byun, D.-J.; Nomura, K. Tuning the active species from syndiospecific styrene polymerisation to ethylene/styrene copolymerisation by (aryloxo)(cyclopentadienyl)titanium complexes–MAO catalysts. *Dalton Trans*. **2007**, (18), 1802−1806. doi.org/10.1039/B701003F
182. Nomura, K.; Komatsu, T.; Imanishi, Y. Polymerization of 1-hexene, 1-octene catalyzed by Cp′TiCl2(O-2,6-$iPr_2C_6H_3$)–MAO system: Unexpected increase of the catalytic activity for ethylene/1-hexene copolymerization by (1,3-$^tBu_2C_5H_3$)$TiCl_2$(O-2,6-$^iPr_2C_6H_3$)–MAO catalyst system. *J. Mol. Catal. A: Chem.* **2000**, *152* (1–2), 249–252. doi.org/10.1016/S1381-1169(99)00388-X
183. Yi, J.; Nakatani, N.; Tomotsu, N.; Nomura, K.; Hada, M. Theoretical study of reaction mechanism for half-titanocene-catalyzed styrene polymerization, ethylene polymerization, and styrene-ethylene copolymerization: Roles of the neutral Ti(III) and the cationic Ti(IV) species. *Organometallics* **2021**, *40* (6), 643–653. doi.org/10.1021/acs.organomet.0c00715
184. Jantawan, K.; Groth, L.; Frank, R.; Chatchaipaiboon, K.; Tamm, M.; Nomura, K. Half-titanocenes bearing unsymmetric imidazolin-2-iminato ligand that exhibit efficient cyclic olefin incorporation in ethylene copolymerization. *ACS Polym. Au* submitted revision.